

1 **Quantifying the relative importance of greenhouse gas emissions from current and future**  
2 **savanna land use change across northern Australia**

3

4 Bristow M.<sup>1,2</sup>, Hutley L.B.<sup>1</sup>, Beringer J.<sup>3</sup>, Livesley S.J.<sup>4</sup>, Edwards A.C.<sup>1</sup>, Arndt S.K.<sup>4</sup>

5

6

7 <sup>1</sup>School of Environment, Research Institute for the Environment and Livelihoods, Charles Darwin  
8 University, NT, Australia, 0909

9 <sup>2</sup>Department of Primary Industry and Fisheries, Berrimah, NT, Australia, 0828

10 <sup>3</sup>School of Earth and Environment, The University of Western Australia, Crawley, WA, Australia,  
11 6009

12 <sup>4</sup>School of Ecosystem and Forest Sciences, The University of Melbourne, Burnley, Victoria,  
13 Australia, 3121

14

15 *Correspondence to:* Lindsay B. Hutley (lindsay.hutley@cdu.edu.au)

16

17 **Keywords:** Deforestation, clearing, eddy covariance, savanna burning, fire emissions

18

## 1 **Abstract**

2 Clearing and burning of tropical savanna leads to globally significant emissions of greenhouse  
3 gases (GHG), however there is large uncertainty relating to the magnitude of this flux. Australia's  
4 tropical savannas occupy the northern quarter of the continent, a region of increasing interest for  
5 further exploitation of land and water resources. Land use decisions across this vast biome have the  
6 potential to influence the national greenhouse gas budget. To better quantify emissions from  
7 savanna deforestation and investigate the impact of deforestation on national GHG emissions, we  
8 undertook a paired site measurement campaign where emissions were quantified from two tropical  
9 savanna woodland sites; one that was deforested and prepared for agricultural land use, and a  
10 second analogue site that remained uncleared for the duration of a 22 month campaign. At both  
11 sites, net ecosystem exchange of CO<sub>2</sub> was measured using the eddy covariance method.  
12 Observations at the deforested site were continuous before, during and after the clearing event,  
13 providing high resolution data that tracked CO<sub>2</sub> emissions through nine phases of land use  
14 change. At the deforested site, post-clearing debris was allowed to cure for six months and was  
15 subsequently burnt, followed by extensive soil preparation for cropping.

16 During the debris burning, fluxes of CO<sub>2</sub> as measured by the eddy covariance tower were  
17 excluded. For this phase, emissions were estimated by quantifying on-site biomass prior to  
18 deforestation and applying savanna-specific emission factors to estimate a fire-derived GHG  
19 emission that included both CO<sub>2</sub> and non-CO<sub>2</sub> gases. The total fuel mass that was consumed during  
20 the debris burning was 40.9 Mg C ha<sup>-1</sup> and included above- and below- ground woody biomass,  
21 coarse woody debris, twigs, leaf litter and C<sub>4</sub> grass fuels. Emissions from the burning were added to  
22 the net CO<sub>2</sub> fluxes as measured by the eddy covariance tower for other post-deforestation phases to  
23 provide a total GHG emission from this land use change.

24 The total emission from this savanna woodland was 148.3 Mg CO<sub>2</sub>-e ha<sup>-1</sup> with the debris  
25 burning responsible for 121.9 Mg CO<sub>2</sub>-e ha<sup>-1</sup> or 82% of the total emission. The remaining emission

1 was attributed to CO<sub>2</sub> efflux from soil disturbance during site preparation for agriculture (10% of  
2 the total emission) and decay of debris during the curing period prior to burning (8%). Over the  
3 same period, fluxes at the uncleared savanna woodland site were measured using a second flux  
4 tower and over the 22 month observation period, cumulative NEE was a net carbon sink of -2.1 Mg  
5 C ha<sup>-1</sup>, or -7.7 Mg CO<sub>2</sub>-e ha<sup>-1</sup>.

6 Estimated emissions for this savanna type were then extrapolated to a regional scale to 1)  
7 provide estimates of the magnitude of GHG emissions from any future deforestation and 2)  
8 compare with GHG emissions from prescribed savanna burning that occurs across north Australian  
9 savanna every year. Emissions from current rate of annual savanna deforestation across north  
10 Australia was double that of reportable (non-CO<sub>2</sub> only) savanna burning. However, if the total GHG  
11 emission is accounted, CO<sub>2</sub> plus non-CO<sub>2</sub> emissions, burning emissions are an order of magnitude  
12 larger than that arising from savanna deforestation. We examined a scenario of expanded land use  
13 that required additional deforestation of savanna woodlands over and above current rates. This  
14 analysis suggested that significant expansion of deforestation area across the northern savanna  
15 woodlands could add an additional 3% to Australia's national GHG account for the duration of the  
16 land use change. This bottom-up study provides data that can reduce uncertainty associated with  
17 land use change for this extensive tropical ecosystem and provide an assessment of the relative  
18 magnitude of GHG emissions from savanna burning and deforestation. Such knowledge can  
19 contribute to informing land use decision making processes associated with land and water resource  
20 development.

21

## 1 **1.0 Introduction**

2 An increase in greenhouse gas (GHG) emissions through human-related activities is leading to  
3 rapid change in the climate system (IPCC 2013). It is therefore crucial to obtain data describing the  
4 net GHG balance at regional to global scales to better characterise anthropogenic forcing of the  
5 atmosphere (Tubiello et al., 2015). Emissions from land-use change (LUC) are the integral of  
6 ecosystem transformations that can include emissions from deforestation and conversion to  
7 agriculture, logging and harvest activity, shifting cultivation, as well as regrowth sinks following  
8 harvest and/or abandonment of previously cleared agriculture lands (Houghton et al. 2012). At  
9 present, LUC emits  $0.9 \pm 0.5 \text{ Pg C y}^{-1}$  to the atmosphere, which is approximately 10% of  
10 anthropogenic carbon emissions (Le Quéré et al., 2014). Data sources and methods used to estimate  
11 LUC emissions are diverse. These include census-based historical land use reconstructions and land  
12 use statistics, satellite estimates of biomass change through time (Baccini et al., 2012), satellite  
13 monitored fire activity and burn area estimates associated with deforestation (van der Werf et al.,  
14 2010). In addition, there is increasing use of ecosystem models coupled with remote sensing to  
15 estimate emissions from LUC (Galford *et al.* 2011).

16 Emissions associated with the LUC sector have the highest degree of uncertainty given the  
17 complexity of processes involving net emissions and Houghton et al. (2012) assessed this  
18 uncertainty at  $\sim 0.5 \text{ Pg C y}^{-1}$ , which is of the same order of magnitude as the emissions themselves.  
19 Uncertainties in estimating GHG emissions arising from savanna clearing, associated debris burning  
20 and conversion to agriculture are greater than those for tropical forests (Fearnside et al., 2009). It is  
21 important to quantify the emissions and their uncertainties in savannas particularly because tropical  
22 savanna woodland and grasslands occupy a large area globally ( $27.6 \text{ million km}^2$ ), greater than  
23 tropical forest ( $17.5 \text{ million km}^2$ , Grace et al., 2006). Deforestation and associated fire from these  
24 biomes are the largest contributors to global LUC emissions (Le Quéré et al., 2014). Much of these  
25 GHG emissions are from the Brazilian Amazonia, an agricultural area that has been expanding

1 since the 1990s. However, over the last decade, the rate of tropical forest deforestation in this region  
2 has decreased from 16,000 km<sup>2</sup> in early 2000s to ~6,500 km<sup>2</sup> by 2010 (Lapola et al., 2014), but at  
3 the expense of the Brazilian cerrado, a vast savanna biome of some 2.04 million km<sup>2</sup>, where  
4 clearing rates have been maintained (Ferreira et al., 2013, 2016; Galford et al., 2013). Given the  
5 suitability of the cerrado topography and soils for mechanized agriculture, the Cerrado may become  
6 the principal region of LUC in Brazil (Lapola et al., 2014).

7 North Australia is one of the world's major tropical savanna regions, extending some 1.93  
8 million km<sup>2</sup> across north-west Western Australia, the northern half of the Northern Territory and  
9 Queensland (Fisher and Edwards, 2015). This biome occupies approximately one quarter of the  
10 Australian continent and since European arrival, 5% has been cleared for improved pasture,  
11 horticulture and cropping (Landsberg et al. 2011), making it one of least disturbed savanna regions  
12 in the world (Woinarski et al., 2007). However, this small percentage equates to a substantial area  
13 of 9.2 million hectares and LUC and associated economic development in northern Australia is a  
14 government imperative and this is likely to involve expansion and intensification of grazing,  
15 irrigated cropping, horticulture and forestry (Committee on Northern Australia, 2014). Drivers of  
16 this potential expansion in food and fibre production include the exploitation of growing markets of  
17 Asia as well as domestic factors such as the perception that land and water resources of north  
18 Australia can provide a future agricultural resource base to offset the expected declines in  
19 agricultural productivity in southern Australia due to adverse impacts of climate change (Steffan  
20 and Hughes, 2013).

21 Historically, intensive agricultural developments in northern Australia have been implemented  
22 based on limited scientific knowledge with dysfunctional policy and market settings, and as a result  
23 there has been limited success (Cook, 2009). Future expansion needs to be underpinned by sound  
24 understanding of the consequences of regional scale land transformation on carbon and water  
25 budgets and GHG emissions. Any significant expansion in northern agricultural production would

1 require clearance of native savanna vegetation, with unknown increases in GHG emissions. Most  
2 LUC studies occur at catchment, regional or biome scales (Houghton et al., 2012) and are not  
3 underpinned by good understanding of underlying processes. However, there are an increasing  
4 number of plot-scale studies using eddy covariance and chamber methods to provide direct  
5 measures of net GHG fluxes from contrasting land uses (Lambin et al., 2013). These studies  
6 typically compare microclimate and fluxes of GHGs from pastures and/or crops with adjacent forest  
7 ecosystems under a range of management conditions (e.g. Anthoni et al. 2004; Zona et al. 2013) or  
8 natural grasslands and different cropping types (e.g. Zenone et al., 2011). In tropical regions, there  
9 is a focus on transitions from forest to pasture and from forest to crops for food or bioenergy  
10 production (Galford et al., 2011; Wolf *et al.* 2011; Sakai *et al.* 2004).

11 There are few studies that directly measure GHG emissions and sinks prior to, during and after  
12 LUC at a single site. Land use change can involve rapid changes in net GHG emissions over  
13 varying temporal scales (minutes, hours, and seasonal cycles) and continuous flux measurements  
14 are essential to capture the magnitude of these events (Hutley et al. 2005). However, there are no  
15 direct observations of emissions from savanna clearing in northern Australia, contributing to the  
16 uncertainty associated with the LUC sector in Australia's national GHG accounts (Commonwealth  
17 of Australia, 2015a).

18 Our objective is to provide a comprehensive assessment of GHG emissions associated with  
19 savanna clearing. Our aims are to 1) quantify the typical rates of CO<sub>2</sub> exchange of intact tropical  
20 savanna and make comparative measurements from an analogue site that was to be cleared, 2)  
21 quantify CO<sub>2</sub> fluxes before, during and after a clearing event, 3) estimate both CO<sub>2</sub> and non-CO<sub>2</sub>  
22 (CH<sub>4</sub> and N<sub>2</sub>O) GHG emissions arising from burning of cleared debris and 4) quantify ecosystem  
23 scale GHG balance for this land use conversion and compare with emissions from savanna fire, a  
24 significant source of GHG emissions across north Australia.

25

## 1 **2.0 Methods**

2 In this study we used a paired site approach, where concurrent fluxes of CO<sub>2</sub>, water vapour and  
3 energy were measured using eddy covariance towers from an uncleared savanna woodland site and  
4 a similar savanna woodland site on the same soil type that was to be cleared, burnt and prepared for  
5 agricultural production. Fluxes of CO<sub>2</sub> were monitored for 161 days prior to clearing at both sites  
6 with observations continuing during the clearing event (deforestation) and for another 507 days  
7 through phases of woody debris and grass curing, burning and soil preparation through raking and  
8 ploughing. The entire observation period was 668 days. Flux observations of net CO<sub>2</sub> exchange  
9 were combined with on-site biomass measurements and regionally calibrated pyrogenic emissions  
10 factors to estimate emissions of CO<sub>2</sub>, CH<sub>4</sub> and N<sub>2</sub>O (Meyers et al. 2012, Commonwealth of  
11 Australia, 2015b) from burning of the cleared debris that was a key component of the land  
12 conversion. Fire derived emissions were combined with net CO<sub>2</sub> fluxes from the land conversion  
13 phases to provide a total net emission in units of CO<sub>2</sub>-e for this LUC. In this paper, we use the term  
14 deforestation to describe 'savanna clearing'. Deforestation is defined under Australia's National  
15 Greenhouse Accounting system as the loss of forest/woodland cover due to direct human-induced  
16 actions that fails to regenerate cover via natural regrowth or restoration planting (Commonwealth of  
17 Australia, 2015a).

### 18 **2.1 Study sites**

19 Both savanna woodland sites were located within the Douglas-Daly River catchment  
20 approximately 300 km south of Darwin, Northern Territory (Fig. 1). Both sites are OzFlux sites  
21 ([www.ozflux.org.au](http://www.ozflux.org.au)), with flux observations ongoing at the uncleared (UC) savanna site since 2007  
22 (Beringer et al. 2016; Beringer et al., 2011; Hutley et al., 2011). OzFlux is the regional Australian  
23 and New Zealand flux tower network that aims to provide continental-scale monitoring of CO<sub>2</sub>  
24 fluxes and surface energy balance to assess trends and improve predictions of Australia's terrestrial  
25 biosphere and climate (Beringer et al., 2016). The UC site is broadly representative of Australian

1 tropical savanna woodland found on deep, well drained sandy loam soils at sites with ~1000 mm  
2 MAP (Table 1). The cleared savanna site (CS) was carefully selected to ensure the vegetation and  
3 soils were as similar to the UC site as possible, and with topography suitable for eddy covariance  
4 measurements.

5 Both sites were classified as savanna woodland (type 4B2, Aldrick and Robinson 1972,  
6 1:50,000 mapping) with an overstorey cover of 30%, equivalent to the 'Eucalypt woodland' Major  
7 Vegetation Group (MVG) of the National Vegetation Information System (NVIS, Commonwealth  
8 of Australia, 2003). The sites were dominated by an overstorey of *Eucalyptus tetradonta* (F.  
9 Muell.), *Corymbia latifolia* (F. Muell.). Soils at both the UC and CS sites were red kandosols of the  
10 haplic mesotrophic great group (Isbell, 2002), characterised as deep, sandy-loams (Table 1). The  
11 long-term mean annual precipitation (MAP) ( $\pm$  SD) at the UC site was estimated at  $1180 \pm 225$  mm  
12 (1970-2012, Australian Water Availability Project (AWAP), [www.csiro.au/awap](http://www.csiro.au/awap)), similar to the CS  
13 site at  $1107 \pm 342$  mm (1985-2013, Bureau of Meteorology station, Tindal, NT). Slopes at both sites  
14 were  $< 2\%$  with a fetch of ~1.5 km at the UC site and ~1 km at the CS site. At both sites, 23 m  
15 guyed masts were installed to support eddy covariance instruments at 21.5 m above-ground. The  
16 tower at the CS site was moved three times to ensure adequate fetch was maintained according to  
17 seasonal wind direction during clearing and phases of the land use conversion. Instrument height  
18 was also adjusted given the height of the surface post-clearing and during the soil tillage phase  
19 (Table 2).

20 Satellite-derived burnt area mapping is available across north Australia at 250 m resolution  
21 (North Australian Fire Information system (NAFI), [www.firenorth.org.au](http://www.firenorth.org.au)) and indicated that fires  
22 had occurred within the flux footprint of the UC flux tower in 5 out of the last 13 years (2000-  
23 2013), whereas no fires had occurred within the footprint of the CS site. The average fire return  
24 time for the entire Australian savanna biome is 3.1 years (Beringer et al., 2015).

## 25 **2.2 Flux measurements and data processing**



1 Eddy covariance systems at both sites consisted of CSAT3 3-D ultrasonic anemometers  
2 (Campbell Scientific Inc., Logan, USA) and a LI-7500 open-path CO<sub>2</sub> / H<sub>2</sub>O analysers (Licor Inc.,  
3 Lincoln, USA). Flux variables were sampled at 10 Hz and covariances stored every 30 minutes. The  
4 LI-7500 gas analysers were calibrated at approximately six month interval for the duration of the  
5 data collection period and were highly stable. Mean daily rainfall, air temperature, relatively  
6 humidity, soil heat flux ( $F_g$ , W m<sup>-2</sup>) and volumetric soil moisture ( $\theta_v$ , m<sup>3</sup> m<sup>-3</sup>) from surface to 2.5 m  
7 depths were measured at both sites. The radiation balance was measured using a CNR4 net  
8 radiometer ( $F_n$ , W m<sup>-2</sup>) (Kipp and Zonen, Zurich).

9 Thirty minute covariances were stored using data loggers (CR3000, Campbell Scientific,  
10 Logan) and data post processing and quality control was undertaken using the OzFluxQC system as  
11 described by Isaac et al. (2016). In this system, data are processed through three levels; Level 1 is  
12 the raw data as collected by the data logger, Level 2 are quality-controlled data and Level 3 are post  
13 processed and corrected but not gap-filled data. Quality control measures at Level 2 include checks  
14 for plausible value ranges, spike detection and removal, manual exclusion of date and time ranges  
15 and diagnostic checks for all quantities involved in the calculations to correct the fluxes. Quality  
16 checks make use of the diagnostic information provided by the sonic anemometer and the infra-red  
17 gas analyser. Level 3 post processing includes 2-dimensional coordinate rotation, low- and high-  
18 pass frequency correction, conversion of virtual heat flux to sensible heat flux ( $F_h$ , W m<sup>-2</sup>) and  
19 application of the WPL correction to the latent heat ( $F_e$ , W m<sup>-2</sup>) and CO<sub>2</sub> fluxes ( $F_c$ ) (Isaac et al.,  
20 2016). Level 3 data also include the correction of the ground heat flux for storage in the layer above  
21 the heat flux plates (Mayocchi and Bristow, 1995).

22 Gap filling of meteorology and fluxes along with flux partitioning of net ecosystem  
23 exchange (NEE) into gross primary productivity (GPP) and ecosystem respiration ( $R_e$ ) was  
24 performed on the Level 3 data using the Dynamic INtegrated Gap filling and partitioning for Ozflux  
25 (DINGO) system as described by Beringer et al., (2016b). In summary, DINGO gap fills

1 meteorological variables (air temperature, specific humidity, wind speed and barometric pressure)  
2 using nearby Bureau of Meteorology (BoM, [www.bom.gov.au](http://www.bom.gov.au)) automatic weather stations that  
3 were correlated with tower observations. All radiation streams were gap-filled using a combination  
4 of MODIS albedo products (MOD09A1) and BoM gridded global solar radiation and gridded daily  
5 meteorology from the Australian Water Availability Project (AWAP) data set (Jones et al. 2009).  
6 Precipitation was gap-filled using either nearby BoM stations or AWAP data. Soil temperature and  
7 moisture were filled using the BIOS2 land surface model (Haverd et al., 2013) run for each site and  
8 forced with BoM or AWAP data. Energy balance closure was examined using standard plots of  
9  $F_h + F_e$  vs  $F_n - F_g$  using 30 minute flux data from both sites (data not shown). For the CS site, closure  
10 was examined using data grouped according to the nine LUC phases as given in Table 2. For the  
11 UC site, all 30 minute data from 2007-2015 was used.

12 Gap filling of fluxes was undertaken using DINGO that uses an Artificial Neural Network  
13 (ANN) model following Beringer et al. (2007). Model training uses gradient information in a  
14 truncated Newton algorithm. NEE and fluxes of sensible, latent and ground heat fluxes were  
15 modelled using the ANN with incoming solar radiation, VPD, soil moisture content, soil  
16 temperature, wind speed and MODIS EVI as inputs. The ustar threshold for each site was  
17 determined following Reichstein *et al.* (2005) and night time observations below the ustar threshold  
18 were replaced with ANN modelled values of  $R_e$  using soil moisture content, soil temperature, air  
19 temperature and MODIS EVI as inputs. The ANN  $R_e$  model was then applied to daylight periods to  
20 estimate daytime respiration and GPP was calculated as the difference between NEE and  $R_e$ . For  
21 data collected at the CS site, a unique ANN model was developed for each LUC phase given the  
22 differing canopy and microclimatology of each phase. At each site, daily NEE,  $R_e$  and GPP were  
23 calculated for each day of each phase.

### 24 **2.3 Leaf area index**

1 Canopy leaf area index (LAI) at the CS site in the surrounding intact savanna was measured  
2 using a 180° hemispherical lens (Nikon 10.5 mm, f/2.8) after Macarlane et al. (2007). Three  
3 savanna transects were photographed seasonally on 9 occasions over 2.1 years from the pre-clearing  
4 phase (October 2011) to December 2013. Along each 100 m transect, 11 hemispherical pictures  
5 were taken at 10 m intervals (33 photos for each measure occasion). At both sites the LAI was also  
6 estimated using MODIS Collection 5 LAI (MOD15A2) for a 1 km pixel around each tower. The 8-  
7 day product was interpolated to daily time series using a spline fit. Only MODIS values with a  
8 quality flag of 0 for FparLai\_QC were used in the estimate indicating the main algorithm was used  
9 ([lpdaac.usgs.gov/sites/default/files/public/modis/docs/MODIS-LAI-FPAR-User-Guide.pdf](http://lpdaac.usgs.gov/sites/default/files/public/modis/docs/MODIS-LAI-FPAR-User-Guide.pdf)).

## 10 **2.4 Land use conversion**

11 The specific sequence and timing of clearing, burning and land preparation phases are given in  
12 Table 2. Conversion of woodland to agricultural land in northern Australia is typically achieved by  
13 pulling trees over using large chains held under tension between two bulldozers. Clearing occurs at  
14 the end of the wet season when soil moisture is still high and soil strength low as under these  
15 conditions trees are easily pulled over, with a large fraction of the tree root mass extracted when  
16 pulled. At the CS site, 295 ha of savanna were deforested between 2 and 6 March 2012 using this  
17 technique. A permit for this land conversion had been issued by the regional land management  
18 agency following an impact assessment and erosion control planning. Chains were under tension  
19 and intercepted tree boles 0.1- 0.2 m height above the ground which assisted in pulling the trees and  
20 limited damage to the soil surface. As a result, grasses, woody re-sprouts and shrubs of the  
21 understorey remained largely intact following deforestation (Plate 1a). Mechanised ripping of soil  
22 to 60 cm depth was also undertaken to remove remaining coarse root material.

23 A cost-effective method of removing cleared vegetation is curing (drying) and subsequent  
24 burning and the land managers at the CS site left debris onsite to for 5 months through the dry  
25 season (March to August, 2011). Burning of debris occurred over a 22 day period in the late dry

1 season, August 2012 (Plate 1b), a period of consistent southerly trade winds of low relative  
2 humidity (10-20%, BoM, Tindal station, NT). Prior to ignition, 100 m fire breaks were installed  
3 around the entire 295 ha block and then lit in blocks of ~80 ha in size. There was an initial ignition  
4 of the fine and coarse fuels (grasses, litter and twigs, defined below) and woody debris (heavy  
5 fuels). Heavy fuels that were not completely consumed following the initial burn were then stock-  
6 piled in rows ~1-2 m in height and re-ignited until the fuel was consumed (Plate 1c). Inspection of  
7 debris post fire suggested ~5% of fine fuels remained as ash and ~10% of the heavy fuels remained  
8 as charcoal, which were subsequently incorporated into the top soil on during soil bed preparation  
9 (Plate 1d).

## 10 **2.5 GHG emissions from debris burning**

11 Emissions of CO<sub>2</sub>, CH<sub>4</sub> and N<sub>2</sub>O from the debris burning were estimated following the  
12 approach as outlined in the IPCC Good Practice Guidelines (IPCC 2003), which uses country or  
13 region specific emission factors for fire activity (indicated by burnt area) and the mass of fuel  
14 pyrolised to estimate the emission of each trace gas. This approach is well developed for the fire  
15 regime of north Australian savanna and is described by Russell-Smith et al. (2013) and Murphy et  
16 al. (2015a). These authors describe a novel GHG emissions abatement methodology for savannas  
17 burning that combines indigenous fire practices with an emissions accounting framework, the  
18 Emissions Abatement through Savanna Fire Management (Commonwealth of Australia 2015b,  
19 [www.comlaw.gov.au/Series/F2013L01165](http://www.comlaw.gov.au/Series/F2013L01165)). This methodology is a legislative instrument that  
20 establishes procedures for abatement projects for prescribed savanna burning and defines emission  
21 factors for four fuel classes; fine (grass and litter < 6 mm diameter fragments), coarse (6 mm–5 cm),  
22 heavy (>5 cm diameter) and shrubs fuels (Russell-Smith et al., 2013). Emissions of GHGs are  
23 estimated based on vegetation type, fuel mass per area for each fuel type, burn area, the burning  
24 efficiency (BEF) for each fuel type, defined as the mass of fuel exposed to fire that is pyrolised, the  
25 fuel carbon content (%), elemental C:N ratios and emission factors (EF) for each GHG (CO<sub>2</sub>, CH<sub>4</sub>

1 and N<sub>2</sub>O) and global warming potentials for each gas. Across north Australian savanna, values for  
2 BEFs and EFs have been determined for both high (>1000 mm MAP) and low precipitation zones  
3 (1000-600 mm MAP) and for both early and late dry season fires, which are fires occurring after 1  
4 August which typically have higher intensity and combustion efficiencies than early dry season  
5 fires (Russell-Smith et al. 2013).

6 We used these definitions of vegetation fuel type (woodland savanna with mixed grass) and  
7 associated EF, carbon contents, N:C ratio values as defined in the methodology to estimate GHG  
8 emissions from the debris fire using the following equation;

$$9 \quad E = \sum_i (FL_j \times BEF_j \times CC_j \times N:C_j \times EF_{i,j} \times GWP_i) \quad \text{Equation 1;}$$

10 where E is the sum of emissions in Mg CO<sub>2</sub>-e ha<sup>-1</sup> for each GHG *i* (CO<sub>2</sub>, CH<sub>4</sub>, and N<sub>2</sub>O), FL<sub>*j*</sub> is the  
11 fuel load for fuel type *j* (fine, coarse, heavy) in Mg C ha<sup>-1</sup>, BEF<sub>*j*</sub> is the burning efficiency factor, CC<sub>*j*</sub>  
12 is the fractional carbon content, N:C<sub>*j*</sub> is the fuel nitrogen to carbon ratio (for N<sub>2</sub>O emissions), EF<sub>*i,j*</sub> is  
13 the emission factor for GHG *i* and fuel type *j* and GWP<sub>*i*</sub> is the global warming potential for each  
14 GHG *i* (after Commonwealth of Australia, 2015b). The debris fire differed from a typical savanna  
15 fire in that there was a significantly higher heavy fuel load present and it was of high intensity  
16 which consumed the vast majority of fuel (Plate 1c,d), reflected in the assumed BEFs we used. The  
17 fire-derived emissions were combined with tower-derived NEE data from the post-clearing phases  
18 (Table 3) to give a total emission in CO<sub>2</sub>-e for this LUC.

## 19 **2.6 Quantifying fuel loads**

20 To accurately quantify emissions from the debris fire, fine, coarse and heavy fuels were  
21 estimated using plots and transects established across the 295 ha deforestation area. For fine fuels,  
22 six 100 m transects were randomly located and at 20 m intervals along each transect, all fine (grass,  
23 woody litter) and coarse (twigs, sticks) fuels were harvested from 1 m<sup>2</sup> quadrats, dried and weighed  
24 to give a mean fine and coarse fuel mass for the site. We assigned on-site coarse woody debris

1 (CWD), above-ground and below-ground biomass estimates to the heavy fuel class (>5 cm diameter  
2 fragments). To quantify CWD, an additional six 100 m transects were randomly located across the  
3 deforestation area and along each transect the length and diameter of all intersected CWD fragments  
4 were recorded to estimate fragment volume. In these savannas, large fragments (>10 cm diameter)  
5 are frequently hollowed from the action of termites and fire and the diameter and length of the  
6 annulus of such fragments were measured to estimate this missing volume. In addition, large  
7 fragments that were tapered were treated as a frustum of a cone and a second diameter was taken at  
8 the fragment end to improve volume estimation. Fragment volumes were calculated and converted  
9 to mass using rot classes (RC) and associated wood densities ( $\text{g cm}^{-3}$ ). Five rot classes (RC) were  
10 defined and assigned to each CWD fragment to capture the decay gradient of fragments. These were  
11 defined as recently fallen, solid wood (RC1), solid wood with or without branches present but with  
12 signs of aging (RC2), obvious signs of weathering, still solid wood, bark may or may not be present  
13 (RC3), signs of decay with the wood sloughed and friable (RC4) and severely decayed fragments  
14 with little structural integrity remaining (RC5). A wood density was assigned to each RC and  
15 species (where identifiable) after Rose (2006) and Brown (1997) to provide an accurate estimate of  
16 CWD mass that included decay and hollowing. For the dominant *Eucalyptus* and *Corymbia* species  
17 wood densities ranged from  $0.7 \text{ g cm}^{-3}$  (RC1) to  $0.56 \text{ g cm}^{-3}$  (RC 5).

18 Above-ground biomass was quantified by surveying all woody plants >1.5 m in height or > 2  
19 cm DBH across eight 50 x 50 m plots. All woody individuals were identified to species and stem  
20 diameter at 1.3 m height (DBH) and tree height were measured. Region specific allometric  
21 equations are available for tree species found at the CS site (Williams et al., 2005) and these were  
22 used to estimate above-ground biomass for each individual tree and shrub based on DBH and  
23 height. Below-ground biomass was calculated using the root:shoot ratio estimate of Eamus et al.  
24 (2002) for these savanna stands which was 0.38. These trees have large lateral roots in the top 30  
25 cm of soil, with no tap root and 90% of root biomass is found in the top 50 cm of soil (Eamus et al.

1 2002). As such, we assumed that chaining and bulldozer clearing of all above-ground biomass  
2 followed by soil ripping (ploughing) to 60 cm soil depth, plus mechanised removal of root biomass  
3 associated with tree boles and subsequent burning, resulted in a near-complete removal of both  
4 above- and below-ground woody biomass pools (Plate 1d).

## 5 **2.7 Deforestation and savanna burning emissions at catchment to regional scales**

6 The potential impact of any expanded deforestation across north Australian savanna landscapes  
7 was assessed relative to historic deforestation rates and resultant GHG emissions and arising from  
8 prescribed savanna burning. This land management activity contributes ~3% to Australia's national  
9 GHG emissions (Whitehead et al., 2014) and is 25% of the Northern Territory's annual emissions  
10 (Commonwealth of Australia, 2015a). Annual emissions from these activities (historic and future  
11 savanna deforestation and prescribed burning) were estimated at three spatial scales; 1) catchment,  
12 2) state/territory and 3) regional. Emissions estimates from deforestation and savanna burning were  
13 compiled for 1) the Douglas-Daly River catchment where the UC and CS sites are located (area  
14 57,571 km<sup>2</sup>), a catchment with less than 5% of the native vegetation deforested to date (Lawes et al.  
15 2015) but earmarked for future development; 2) the savanna area of Northern Territory (856,000  
16 km<sup>2</sup>) and 3) the savanna region of north Australia as defined by Fox et al. (2001) with MAP > 600  
17 mm, an area of 1.93 million km<sup>2</sup> (Fig. 1, insert).

18 Emissions of GHG from historic deforestation from the Douglas-Daly catchment were  
19 estimated using our estimates for savanna land conversion combined with satellite-derived annual  
20 deforestation area (1990-2013) as reported by Lawes et al. (2015) for this catchment to give a  
21 catchment scale mean annual estimate of emissions from deforestation in Gg CO<sub>2</sub>-e y<sup>-1</sup>. Annual  
22 deforestation emissions data for the Northern Territory and the north Australian savanna region  
23 were taken from the National Greenhouse Gas Inventory (NGGI) for the same period 1990-2013.  
24 The Department of Environment is responsible for reporting sources of greenhouse gas emissions  
25 and removals by sinks in accordance with UNFCCC Reporting Guidelines on Annual Inventories

1 and the supplementary reporting requirements under the Kyoto Protocol. State and Territory GHG  
2 Inventories are reported for 1990 to 2013 (Commonwealth of Australia, 2015a) and we used data  
3 for the Land Use, Land-Use Change and Forestry sector, Activity A.2 Deforestation. These  
4 emissions are reported for each State, but are not biome based and for our regional savanna  
5 estimate, emissions data for Western Australia, the Northern Territory and Queensland were used  
6 but were calculated using the area within each state that was defined as savanna by Fox et al. (2001,  
7 Fig. 1). Mean annual deforestation emissions from the savanna area of each state and territory  
8 (1990-2013) were summed to calculate a mean ( $\pm$ SD) annual deforestation rate for the north  
9 Australian savanna area (1.92 million km<sup>2</sup>) in Gg CO<sub>2</sub>-e y<sup>-1</sup>.

10 Emissions from savanna burning were calculated using the on-line Savanna Burning Abatement  
11 Tool (SAVBat2, [www.savbat2.net.au](http://www.savbat2.net.au)) using the pre-defined Vegetation Fuel Types (VFTs)  
12 mapping for north Australian savanna (Fisher and Edwards, 2015; Thackway, 2014), both  
13 components of the Emissions Abatement through Savanna Fire Management methodology.  
14 SAVBat2 combines satellite derived burnt area mapping ([www.firenorth.org.au](http://www.firenorth.org.au)) with fuel load  
15 estimates from VFT mapping, GHG emission factors and burn efficiencies to estimate annual  
16 emissions from burn areas. In accordance with IPCC accounting rules, only non-CO<sub>2</sub> emissions are  
17 reported for savanna burning as it is assumed that CO<sub>2</sub> emissions from dry season burning is offset  
18 by re-growth of vegetation (mostly C<sub>4</sub> grasses) in subsequent wet season(s) (IPCC, 1997).  
19 However, for comparisons with deforestation emissions, we calculated emissions of CO<sub>2</sub> as well as  
20 non-CO<sub>2</sub> emissions. SAVBat2 estimates were compiled for the same areas as savanna deforestation  
21 estimates; the Douglas-Daly River catchment, savanna of the NT and north Australian savanna.  
22 Mean annual burning emissions for 1990-2013 were calculated and are reported as non-CO<sub>2</sub> (CH<sub>4</sub>,  
23 N<sub>2</sub>O) and total emissions (CO<sub>2</sub>, CH<sub>4</sub> and N<sub>2</sub>O) in Gg CO<sub>2</sub>-e y<sup>-1</sup>.

## 24 **2.8 Emissions from expanded deforestation across north Australia**



1 Emissions from expanded deforestation across north Australia was estimated by upscaling our  
2 estimate of deforestation emissions per hectare from catchment areas identified as having future  
3 clearing potential. These areas were based on the land use assessment of north Australian  
4 catchments by Petheram et al. (2014) and identified catchments with development potential based  
5 upon surface water storage and proximity of land resources suitable for irrigation development for  
6 agriculture, horticulture or improved pastures. Using these criteria, suitable catchments were  
7 identified in Western Australia (Fitzroy River, Ord Stage 3; 75 000 ha potential area), the Northern  
8 Territory (Victoria, Roper Rivers, Ord Stage 3, Darwin-Wildman River area; 114, 500 ha) and  
9 Queensland (Archer, Wenlock, Normanby, Mitchel Rivers; 120 000 ha). This gives a potential  
10 savanna deforestation area of 311, 000 ha, equivalent to an additional 16% of cleared land over and  
11 above the 1,886,512 ha that has been cleared across the savanna biome since 1990 (Commonwealth  
12 of Australia, 2015a). Projected emissions included mean annual emissions from historic  
13 deforestation rates plus emissions from this expanded deforestation scenario. Expanded  
14 deforestation areas were calculated assuming any such clearing would occur over a five year period  
15 and are reported as non-CO<sub>2</sub> (CH<sub>4</sub>, N<sub>2</sub>O) and total emissions (CO<sub>2</sub>, CH<sub>4</sub> and N<sub>2</sub>O) in Gg CO<sub>2</sub>-e y<sup>-1</sup>.

## 16 **3.0 Results**

### 17 **3.1 Pre-clearing site comparisons**

18 Pre-clearing meteorology, flux observations and energy balance closure for UC and CS sites  
19 were compared (Fig. 2). Mean monthly NEE, R<sub>e</sub> and GPP for each LUC phase for both sites are  
20 given in Table 3. Flux measurements prior to clearing were made for 161 days, a period spanning  
21 the late dry to early wet season transition (September-December) through to the mid-wet season  
22 (January-February, Table 2). Flux data at the CS site were validated by assessing energy balance  
23 closure, with a regression between energy balance components suggesting closure was high with a  
24 slope of 0.91 and an R<sup>2</sup> of 0.95 (n=4778). Site differences for each phase were tested using one-way  
25 ANOVA using daily mean NEE with days as replicates. For Phase 1, mean daily NEE was not

1 significantly different between the two sites during ( $P < 0.64$ ,  $df = 321$ ). Seasonal patterns of  $T_{air}$ ,  
2 VPD (Fig. 2b), LAI (Fig 2c) and C fluxes (NEE, GPP,  $R_e$ , Fig 2d) were similar when both sites  
3 were intact, although precipitation was 340 mm higher at the UC site (Table 3).

4 At both sites, NEE shifted from being a weak sink of less than  $-1 \mu\text{mol CO}_2 \text{ m}^{-2} \text{ s}^{-1}$  during the  
5 late dry season to a net source of  $\text{CO}_2$  during the early wet season (Fig. 2d). During this period,  $R_e$   
6 increased rapidly from  $+2 \mu\text{mol m}^{-2} \text{ s}^{-1}$  to  $+5 \mu\text{mol m}^{-2} \text{ s}^{-1}$  in early October with the onset of wet  
7 season rain, but then remained relatively constant for the remainder of the wet season. As the wet  
8 season progressed, temporal patterns of GPP were similar at both sites and steadily increased to  $-6$   
9 to  $-7 \mu\text{mol m}^{-2} \text{ s}^{-1}$  and remained at this rate until cleared (March 2012).  $R_e$  was relatively stable  
10 during this period and NEE increased to  $-2 \mu\text{mol m}^{-2} \text{ s}^{-1}$  through the wet season (December to  
11 February). Despite the higher precipitation received at the UC site, mean monthly NEE, GPP and  $R_e$   
12 differed by  $< 10\%$  (Table 3, intact canopy phase). Normalising fluxes by MODIS LAI for each site  
13 further reduced differences to 2% (data not shown), suggesting site differences were small and the  
14 UC site provides a suitable control for the CS site.

### 15 **3.2 Fluxes following clearing**

16 Clearing of the 295 ha block commenced on 2 March 2012 and the bulldozers reached the  
17 footprint of the flux tower at  $\sim 0900\text{h}$  local time on 6 March (Fig. 3). As for Phase 1, energy balance  
18 closure of flux tower data for LUC Phases 2 to 4 (post-clearing phases) was high, with a slope  $> 0.9$   
19 and  $R^2 > 0.92$ . Over all phases at the CS site, closure was lower, with a slope of 0.81 ( $R^2 = 0.95$ ,  
20  $n = 26,395$ ), similar to that of the UC site at 0.87 ( $R^2 = 0.93$ ,  $n = 99,998$ ).

21 The four day clearing event occurred during relatively high soil moisture conditions, with  
22 surface (5 cm depth)  $\theta_v$  ranging from 0.08 to  $0.10 \text{ m}^3 \text{ m}^{-3}$  and sub-soil  $\theta_v$  (50 cm depth) ranging  
23 from 0.12 to  $0.14 \text{ m}^3 \text{ m}^{-3}$ . As a result, pre-clearing fluxes were high and NEE reached  $-15 \mu\text{mol CO}_2$   
24  $\text{m}^{-2} \text{ s}^{-1}$  during the middle of the day (Fig. 3). Mean daily NEE for the week prior to clearing was a  
25 net  $\text{CO}_2$  sink of  $-0.60 \pm 0.63 \mu\text{mol m}^{-2} \text{ s}^{-1}$ , and was not significantly different to mean daily NEE at

1 the UC site of  $-0.80 \pm 0.93 \mu\text{mol m}^{-2} \text{s}^{-1}$  (ANOVA,  $P < 0.03$ ). For the three weeks following clearing,  
2 the CS site rapidly became a net source of  $\text{CO}_2$  with a mean daily NEE of  $+4.38 \pm 0.24 \mu\text{mol m}^{-2} \text{s}^{-1}$ ,  
3 with a much reduced diurnal amplitude and no response to precipitation events (Fig 3a,b). High  
4 closure (slope  $> 0.9$ ) was observed during Phases 2 to 4, although this was reduced (slope = 0.75) for  
5 the post-fire and soil preparation, Phases 6-9.

6 Table 3 provides values of precipitation and monthly NEE, Re and GPP for the seven LUC  
7 phases following clearing, namely debris decomposition and curing (153 days), burning (22 days),  
8 wet season regrowth (80 days), followed by soil tillage and preparation of irrigated raised soil beds  
9 (181 days). For each phase, the comparable flux estimate from the UC site is estimated for all post  
10 clearing phases and for the entire observation period. Following clearing, GPP at the CS site was  
11 reduced by a factor of 3.5 when compared to the UC for the same period (March 2012 – January  
12 2013, Table 3). While greatly reduced, GPP still occurred at the CS site during this 13.7 month  
13 period ( $-0.38 \text{ Mg C ha}^{-1} \text{ month}^{-1}$ ), via re-sprouting of felled overstorey and sub-dominant trees and  
14 shrubs, as well as grass germination and growth stimulated by early wet season precipitation  
15 (November 2012-January 2013, 361 mm, Table 3). Ecosystem respiration during this period was  
16 higher at the UC site ( $+1.12 \text{ Mg C ha}^{-1} \text{ month}^{-1}$ ) when compared to the CS site ( $+0.82 \text{ Mg C ha}^{-1}$   
17  $\text{month}^{-1}$ ) and given the large decline in GPP, the CS site was a small net C source at  $+0.51 \text{ Mg C ha}^{-1}$   
18  $\text{month}^{-1}$ , as compared to the UC site which was a weak sink of  $-0.03 \text{ Mg C ha}^{-1} \text{ month}^{-1}$ .

19 Cumulative NEE over all the post-clearing LUC phases was  $+7.2 \text{ Mg C ha}^{-1}$  at the CS site as  
20 compared to a net sink of  $-0.78 \text{ Mg C ha}^{-1}$  at the UC site (Table 3). The temporal dynamics of  
21 cumulative NEE across all LUC phases (note differences in phase duration) is summarised in Fig. 4,  
22 which compares fluxes from both sites for the complete observation period. Three significant  
23 periods of C emission are evident in Fig. 4. Firstly, the clearing event and the subsequent switch  
24 from a C sink to a net source of  $1.9 \text{ Mg C ha}^{-1}$  due to soil disturbance and the decomposition of  
25 biomass. Secondly, this was followed by a reduction in source strength over the dry season of 2012,

1 attributable to a reduction in  $R_e$  during the dry season (2012 dry season pre-burn phase, Table 3).  
2 Thirdly, there were other major emissions attributed to soil tillage and bed preparation in the wet  
3 and dry seasons of 2013, a cumulative net emission of  $+2.75 \text{ Mg C ha}^{-1}$  that occurred over the final  
4 six months (Fig. 4) in preparation for cropping. Over this phase, the UC site was a net sink of  $-0.62$   
5  $\text{Mg C ha}^{-1}$ .

### 6 **3.4 Emissions from debris burning**

7 Table 4 gives fuels loads, BEF, EF, carbon content and N:C ratios for each fuel type used to  
8 estimate the GHG emission from the debris burning. Fuel load was dominated by heavy fuels with a  
9 mean ( $\pm$ SD) above-ground biomass of  $26.9 \pm 7.0 \text{ Mg C ha}^{-1}$  and a range of 14.4 to  $39.3 \text{ Mg C ha}^{-1}$   
10 across the eight biomass plots. The mean below-ground biomass was estimated at  $9.0 \pm 2.4 \text{ Mg C}$   
11  $\text{ha}^{-1}$  and CWD was  $1.4 \pm 0.6 \text{ Mg C ha}^{-1}$ . Fine and coarse fuels were  $1.4 \pm 0.7$  and  $0.5 \pm 1.0 \text{ Mg C ha}^{-1}$   
12 respectively, giving a total fuel mass of  $38.2 \text{ Mg C ha}^{-1}$ . Using these fuel loads with savanna EF  
13 and the BEFs estimated for the site gave an emissions of  $\text{CO}_2$ ,  $\text{CH}_4$  and  $\text{N}_2\text{O}$  for each fuel type and  
14 the emission from debris burning totalled  $121.9 \text{ Mg CO}_2\text{-e ha}^{-1}$ , with 9.5% of this total comprising  
15 non- $\text{CO}_2$  emissions (Table 4).

### 16 **3.5 Total GHG emission**

17 Emissions derived from debris burning needs to be combined with the post-clearing NEE as  
18 measured by the EC system to provide a total GHG emissions estimate from this LUC in units of  
19  $\text{CO}_2\text{-e}$ . The LUC phases following clearing spanned a 502 day period (Table 3), and NEE was  $+7.2$   
20  $\text{Mg C ha}^{-1}$  or  $+26.4 \text{ Mg CO}_2\text{-e ha}^{-1}$ . In comparison, NEE from the UC site over the same period was  
21  $-0.78 \text{ Mg C ha}^{-1}$  or  $-2.9 \text{ CO}_2\text{-e ha}^{-1}$ . Adding NEE from post-clearing phases (Phases 2-9, Table 3) to  
22 emissions from debris burning (Table 4) gave a total emission of  $+148.3 \text{ Mg CO}_2\text{-e ha}^{-1}$  for the CS  
23 site. The  $\text{CO}_2$ -only emission from debris burning plus post-clearing NEE was  $+136.7 \text{ Mg CO}_2 \text{ ha}^{-1}$ ,

1 which was a flux 45 times larger than the observed savanna CO<sub>2</sub> sink at the UC site over the post-  
2 clearing period.

### 3 **3.6 Upscaled and projected emissions from deforestation and savanna burning**

4 Table 5 provides mean ( $\pm$ SD) GHG emissions estimates for savanna burning and deforestation  
5 for 1990-2013. At all spatial scales, annual mean burnt area dwarfed the mean annual land area  
6 deforested. For the Douglas-Daly catchment area, reportable non-CO<sub>2</sub> emissions from savanna  
7 burning were  $577\pm 124$  Gg CO<sub>2</sub>-e y<sup>-1</sup>, almost four times larger than emissions from the mean annual  
8 savanna deforestation rate of  $163\pm 162$  Gg CO<sub>2</sub>-e y<sup>-1</sup>. For the Northern Territory savanna, mean  
9 annual burning emissions were an order of magnitude larger than mean annual deforestation  
10 emissions (Table 4) and two orders of magnitude larger if CO<sub>2</sub> emissions were included. At a  
11 regional scale, the mean annual deforestation rate across the north Australian savanna was  
12  $16,161\pm 5,601$  Gg CO<sub>2</sub> y<sup>-1</sup>, with emissions from Queensland savanna area dominating this amount at  
13  $15,762\pm 5,566$  Gg CO<sub>2</sub> y<sup>-1</sup>. This is double that of the reportable (non-CO<sub>2</sub> only) emission from  
14 prescribed burning at  $6,740\pm 1,740$  Gg CO<sub>2</sub> y<sup>-1</sup> (Table 5).

15 Emissions estimates that include future deforestation rates would be equivalent to savanna  
16 burning, at least for the duration of the additional deforestation. For the Douglas-Daly catchment,  
17 this future emission is estimated at 756 Gg CO<sub>2</sub>-e y<sup>-1</sup> and across the Northern Territory savanna  
18 area, this would be 3,413 Gg CO<sub>2</sub>-e y<sup>-1</sup>, rates of emission that are equivalent to burning emissions  
19 catchment (Douglas-Daly,  $577\pm 124$ ) and state scales (Northern Territory savanna,  $3,490\pm 922$  Gg  
20 CO<sub>2</sub>-e y<sup>-1</sup>). Emissions that include future deforestation rates for the north Australian savanna region  
21 were estimated at 24,393 Gg CO<sub>2</sub>-e y<sup>-1</sup> and would be three times the reportable savanna burning  
22 annual emissions (Table 5).

## 23 **4.0 Discussion**

1 Australia has lost approximately 40% of its native forest and woodland since colonisation  
2 (Bradshaw, 2012), with most of this clearing for primary production in the eastern and south-eastern  
3 coastal region. Attention has now turned to the productivity potential of the largely intact northern  
4 savanna landscapes, which will involve trade-offs between management of land and water resources  
5 for primary production and biodiversity conservation (Adams and Pressey, 2014; Grundy et al.,  
6 2016). Globally and in Australia, savanna fire ecology and fire derived GHG emissions have been  
7 reasonably well researched (Beringer et al., 1995; Cook and Meyer, 2009; Livesley et al., 2011;  
8 Meyer et al., 2012; Walsh et al., 2014; van der Werf et al., 2010) and the impacts of fire on the  
9 functional ecology of Australian savanna has been recently reviewed by Beringer et al. (2015). In  
10 this study, we focussed on savanna deforestation and land preparation for agricultural use. These  
11 phases result in a series of events that may lead to pulsed GHG emissions that would otherwise be  
12 missed or greatly under-estimated by episodic measurements taken at a weekly or monthly  
13 frequency after an initial tree felling event (Neill et al., 2006; Weitz et al., 1998).

14 We used the eddy covariance methodology as it provides a direct and non-destructive  
15 measurement of the net exchange of CO<sub>2</sub> and other GHG gases at high temporal resolution, ranging  
16 from 30 minute intervals to daily, monthly, seasonal and annual estimates. The method is useful as  
17 a full carbon accounting tool as all exchanges of CO<sub>2</sub> from autotrophic and heterotrophic components  
18 of the ecosystem undergoing change are quantified (Hutley et al., 2005). This approach provides  
19 essential data for bottom-up GHG and carbon accounting studies as micrometeorological conditions  
20 and associated fluxes can be tracked through time for the duration of a land use conversion.

21 At the CS site, burning of post-clearing debris comprised 82% of the total emission of 148.4  
22 Mg CO<sub>2</sub>-e ha<sup>-1</sup>, with the remainder attributed to NEE as measured by the flux tower. This flux  
23 comprised significant CO<sub>2</sub> losses via respiration of debris, enhanced soil CO<sub>2</sub> efflux from soil  
24 disturbance and tillage, which was partially offset by net uptake of CO<sub>2</sub> from woody re-sprouting  
25 post-clearing and periods of grass growth following wet season rainfall (Fig. 4). Soil disturbance via

1 ripping, tillage and preparation was responsible for 10% of the CO<sub>2</sub> emission from the conversion.  
2 The EC flux tower was operational during the clearing event, demonstrating the utility of this  
3 method as the switch of the ecosystem from being a net CO<sub>2</sub> sink to being a net source occurred  
4 over a number of hours as the clearing event was completed (Fig. 3). During the LUC phase  
5 changes, there was little evidence of major pulses of CO<sub>2</sub> flux, instead there was a rapid transition  
6 to a new diurnal pattern following the clearing (Fig. 3) or the commencement of soil preparation  
7 (data not shown). This is in contrast to non-CO<sub>2</sub> flux emissions, in particular N<sub>2</sub>O, with short term  
8 emissions often follow disturbance (Grover et al., 2012; Zona et al., 2013) and can be a significant  
9 fraction of annual emissions.

10 The net CO<sub>2</sub> source as measured by the flux tower represents an emission that would be missed  
11 if vegetation biomass density alone was used to estimate LUC emissions, the approach used in  
12 current remote sensing LUC studies at regional and continental scales, data that is the basis of  
13 emissions reporting for the LULUC sector. The total GHG emission we report in this study is more  
14 accurately described as a land conversion, as it includes the oxidation of biomass plus emissions  
15 associated with soil disturbance and tillage required for a conversion to a cropping or grazing  
16 system.

17 The emission estimate from this study does not include non-CO<sub>2</sub> soil derived fluxes of CH<sub>4</sub> and  
18 N<sub>2</sub>O, which can be significant for LUC events in certain ecosystems (Tian et al., 2015). Grover et  
19 al. (2012) compared soil CO<sub>2</sub> and non-CO<sub>2</sub> fluxes from native savanna with young pasture and old  
20 pastures (5-7 and 25-30 years old) in the Douglas-Daly River catchment. Soil emissions of CO<sub>2</sub>-e  
21 were 30% greater on the pasture sites as compared with native savanna sites, with this change being  
22 dominated by increases in CO<sub>2</sub> emission and soil CH<sub>4</sub> exchange shifting from a small net sink to a  
23 small net source at the pasture sites. Non-CO<sub>2</sub> soil fluxes were generally small, especially N<sub>2</sub>O  
24 emissions, although these measurements were made many years after the LUC event and there is  
25 uncertainty as to their relevance for a recently deforested and converted savanna site. An additional

1 pathway for CH<sub>4</sub> and N<sub>2</sub>O emissions in these savannas is via termite activity (Jamali et al., 2011a,  
2 2011b). In our study, termite mounds were abundant across the CS site but were largely destroyed  
3 by clearing and soil preparation, potentially reducing the net non-CO<sub>2</sub> emission following  
4 conversion. Further work is required to quantify these non-CO<sub>2</sub> fluxes not associated with debris  
5 burning to refine our total emission estimate for savanna deforestation.

6 This land conversion represents the loss of decades of carbon accumulation in this mesic  
7 savanna (>1000 mm MAP), ecosystems which are currently thought to be a weak carbon sink  
8 (Beringer et al., 2015). The 8-year ensemble mean NEE for the UC site was  $-0.11 \pm 0.16 \text{ Mg C ha}^{-1}$   
9  $\text{y}^{-1}$  and is representative of a savanna site at a near-equilibrium state in terms of carbon balance  
10 given the low fire frequency (3 in 13 years, Table 1) with high severity fires uncommon (1 in 8  
11 years of flux measurements). The annual increase in tree biomass at this UC site is  $0.6 \text{ t C ha}^{-1} \text{ y}^{-1}$   
12 (Rudge, Hutley, Beringer, unpublished data), and given an above-ground standing biomass of 28 t  
13  $\text{C ha}^{-1}$  suggests a regeneration period of approximately four to five decades after stand replacement  
14 disturbance event such as deforestation for this savanna type.

15 Even after the large pool of carbon is lost following oxidation of biomass, carbon loss may  
16 continue on cleared land via continued soil carbon mineralisation, leading to a slow decline in soil  
17 carbon storage that is frequently reported for forest to cropping LUC (Jarecki and Lal, 2003; Lal  
18 and Follett, 2009). Conversion of forest or woodland to improved pasture grazing may result in  
19 either increases or decreases in soil carbon (Sanderman et al., 2010). Alternatively, it is possible  
20 that carbon sequestration may occur post-clearing via woody regrowth if a cleared site is abandoned  
21 and not further prepared for cultivation. This has actually been a relatively common transition and a  
22 significant sequestration pathway that needs to be included in savanna LUC assessments (Henry et  
23 al. 2015). Admittedly, if savanna cleared land does fully transition to a cropping system, some  
24 fraction of the lost carbon could also be replaced or sequestered by new horticultural or forestry  
25 land uses.



1        There are few detailed, plot scale studies of GHG emissions from savanna clearing in north  
2 Australia. Several studies (Law and Garnett 2009, 2011) used the Full Carbon Accounting Model  
3 (FullCAM Ver 3.0, Commonwealth of Australia, 2015a; Richards and Evans, 2004) to generate  
4 spatial maps of above- and below-ground biomass and soil organic carbon pools across the NT. The  
5 FullCAM model uses spatial and temporal soil, climate, precipitation data with NVIS major  
6 vegetation classes to simulate carbon losses (as GHG emissions) and uptake between the terrestrial  
7 biological system and the atmosphere. Land use change scenarios can be run within the model and  
8 Law and Garnett (2009) examined deforestation emissions from the Eucalypt woodland NVIS  
9 vegetation class, as per UC and CS site classification. Modelled emissions were  $136 \pm 42$  Mg CO<sub>2</sub>-e,  
10 comparable to our deforestation estimate of 121.4 Mg CO<sub>2</sub>-e. Henry et al. (2015) used a life cycle  
11 assessment approach to quantify GHG emissions from LUC associated with beef production in  
12 eastern Australia. Australia's major beef producing areas across central and southern Queensland  
13 and northern central New South Wales were classified into 11 bioregions, with the northern most  
14 bioregion, the northern Brigalow Belt, falling within the savanna biome. Vegetation biomass from  
15 this bioregion was estimated at  $84.7 \pm 7.1$  Mg ha<sup>-1</sup> or  $\sim 41.4$  Mg C ha<sup>-1</sup>, with an emission estimated at  
16 129 Mg CO<sub>2</sub>-e (Henry et al., 2015), similar to the woodland biomass density and resultant emission  
17 with deforestation from the CS site of this study.

18        Our emissions estimate is robust for this vegetation class and can be upscaled and compared  
19 with other land sector activities such as prescribed savanna burning. At a regional scale, current  
20 levels of savanna burning dominate emissions compared to land clearing rates (Table 5). The  
21 cumulative deforestation area across the savanna region since 1990 (1,886,512 ha) is 17 times  
22 smaller than the mean annual savanna burn area (32 Mha, Table 5) as approximately 30 to 70% of  
23 the savanna area is burnt annually (Russell-Smith et al., 2009). Modelling NEP for savanna biome  
24 for 1990-2010 (Beringer et al., 2015; Haverd et al., 2013) suggests the north Australian savanna is  
25 near carbon neutrality, or is a weak source of CO<sub>2</sub> to the atmosphere once regional scale fire  
26 emissions are included. As such, the IPCC assumption that CO<sub>2</sub> emissions from the previous year's

1 burning are recovered by the following year's wet season growth may have some validity for  
2 regional scale GHG accounting. This assumption at plot to catchment scales may not be valid, as  
3 localised interannual variability in rainfall, site history and fire management can result in either net  
4 accumulation or loss of carbon (Hutley and Beringer, 2011; Murphy et al., 2014, 2015b). Assuming  
5 year to year CO<sub>2</sub> emitted from burning is re-sequestered, assessment of the non-CO<sub>2</sub> only emissions  
6 from savanna burning with deforestation is useful. This comparison suggests projected deforestation  
7 emissions (24,393 Gg CO<sub>2</sub>-e y<sup>-1</sup>, Table 5) could be well in excess of current annual burning  
8 emissions (6,740 Gg CO<sub>2</sub>-e y<sup>-1</sup>, Table 5), at least for the period of enhanced clearing, which in this  
9 study we assumed to be five years.

10 In 2013, Australia's total reported GHG emission was 548,440 Gg CO<sub>2</sub>-e and the impact of  
11 expanded savanna deforestation on the national emission can be estimated using data in Table 5  
12 which provide estimates of mean annual emissions from deforestation area, giving a mean annual  
13 deforestation emission per ha averaged for the entire savanna area, which is 221 ±50.8 Mg CO<sub>2</sub>-e  
14 ha<sup>-1</sup> using 1990 to 2013 data (Commonwealth of Australia, 2015a). This value represents a spatially  
15 averaged emission as it is derived from the full range of savanna vegetation types and above-ground  
16 biomass, which across the Northern Territory savanna area ranges from 10 to 70 Mg C ha<sup>-1</sup> (Law  
17 and Garnett, 2011). Assuming this emission per ha, an additional 311, 000 ha of savanna  
18 deforestation, cleared over a five year period, adds 12,099 Gg CO<sub>2</sub>-e y<sup>-1</sup>. For the duration of the  
19 expanded deforestation, this is a 2.2% increase to Australia's nation emission over and above the  
20 historic savanna LUC emissions (16,161 Gg CO<sub>2</sub>-e y<sup>-1</sup>), which are 2.9% of national emissions.  
21 Using our finding from flux tower measurements that a land conversion (deforestation followed by  
22 site tillage and preparation for cultivation) adds an additional 18% of GHG emissions to a  
23 deforestation event, expansion of northern land development could add an additional 3% or 33, 350  
24 Gg CO<sub>2</sub>-e y<sup>-1</sup> to the reportable national GHG emissions for the duration of the expanded  
25 deforestation period.

1 This assessment is subject to a number of uncertainties. Firstly, a component of our emissions  
2 estimate is based on eddy covariance measurements of CO<sub>2</sub> flux, which typically have an error of  
3 10-20% (Aubinet et al., 2012). In this study, energy balance closure suggested fluxes were  
4 underestimated by up to 13% across the entire observation period. Energy balance closure ranged  
5 from <10% flux loss during the intact canopy phase to >20% error during the final three LUC  
6 phases when the flux instruments were at 3 m height measuring net soil CO<sub>2</sub> emissions from the  
7 smoothed, vegetation-free ploughed soil surface during preparation. Secondly, it is difficult to  
8 predict the nature of future deforestation (rate, area, specific location) and the emission comparisons  
9 presented here are indicative only. Catchments selected by Petheram et al. (2014) regarded as  
10 suitable or with potential for future development were based on biophysical properties only, were  
11 unconstrained by the regulatory environment and did not account for conservation and cultural  
12 values placed on identified land and water resources. In addition, challenges to agricultural  
13 expansion in northern Australia include uncertain land and water tenure, high development costs  
14 and lack of existing water infrastructure, logistics and technical constraints, lack of human capital  
15 and distance to markets, all factors that may restrict land clearing. It is well understood that the  
16 availability and cost of water for irrigated, or irrigation assisted agriculture is critical for viable  
17 agriculture in northern Australia (Petheram et al., 2008, 2009). Australian Government policies  
18 currently support small-scale, precinct or project scale approaches, based on well-understood water  
19 and soil resources, where water allocation is capped. The current policy and market instruments are  
20 likely to ensure that development remains measured and restricted, unlike development of previous  
21 decades in other regions of eastern and southern Australia.

22 As a result we used a conservative estimate of potential land suitability area (311, 000 ha over a  
23 five year clearing period), as estimates of assumed clearable area ranging up to 700,000 ha (e.g.,  
24 Douglas-Daly catchment, Adams and Pressey, 2014) or over 1 million ha across north Australia  
25 (Petheram et al. 2014), areas that may be unlikely given capital investment requirements as well as  
26 conservation and cultural considerations. Our comparison with burning emissions is also influenced

1 by the deforestation period we assume. This was based on patterns of historic rates of clearing as  
2 there are periods when deforestation rates have easily exceeded 311,000 ha over five year periods,  
3 particularly in Queensland (Commonwealth of Australia, 2015a) and a longer duration of  
4 deforestation reduces the impact on annual national GHG accounting.

5 There is also uncertainty arising from our emissions from debris burning. Russell-Smith et al.  
6 (2009) estimated errors associated with emissions estimates from the Western Arnhem Land Fire  
7 Abatement (WALFA) project, a savanna burning based GHG abatement scheme operating in the  
8 Northern Territory. This is a project area of the 23,893 km<sup>2</sup> consisting of a wide range vegetation  
9 types including open-forest and woodland savanna and sandstone heaths in escarpment areas.  
10 Russell-Smith et al. (2009) estimated the accountable emissions from savanna burning at  $272 \pm 100$   
11 Gg CO<sub>2</sub>-e y<sup>-1</sup> (95% CI), an error of 30–35% of the mean. Uncertainty was ascribed to errors in  
12 remotely sensed burn area mapping, fuel load estimation, spatial variation of fire severity, errors in  
13 BEF for each fuel class and EFs. At the spatial scale of our study area, there were no uncertainties  
14 with the burnt area, vegetation structure or fuel type classification, and we used site-specific fuel  
15 load estimations used in our calculations, all of which would reduce the error associated with our  
16 fire emissions estimate. Russell-Smith et al. (2009) also reported low coefficients of variability  
17 (CV%) of for BEFs across fine, coarse and heavy fuel types for high severity fires, ranging from 0.3  
18 to 11% and 2% CV for EFs for CH<sub>4</sub> and N<sub>2</sub>O. Site specific sources of error include high spatial  
19 variability of on-site fuel loads which had a CV% of ~70% (Table 4) and uncertainty associated  
20 with the BEF we assumed for coarse and heavy fuel loads (0.9), which is higher than that derived  
21 for late dry season savanna fires (0.36, 0.31 respectively, Russell-Smith et al. 2009). This value was  
22 assumed as repeat burning of coarse and heavy fuels ensured ~10% of biomass remained as ash and  
23 charcoal at the CS site. This assumed BEF is also consistent with FullCAM (4.00.3) BEF of 0.98  
24 for forest fire with 100% of trees killed, although this is setting is based on Surawski et al. (2012)  
25 who found little empirical evidence for BEF for stand-replacement fires. However, given the

1 detailed on-site measurements of fuel load, error in our fire-derived emissions would be of the order  
2 of 20% or less.

### 3 **5.0 Conclusions**

4 While GHG emissions from savanna deforestation are dominated by debris burning, emissions  
5 from soil tillage and soil bed preparation is likely to be 20% of the total emission, suggesting  
6 satellite-based emissions based on oxidation of cleared vegetation alone do not capture all phases of  
7 LUC prior to cultivation. Savanna burning, using the area as defined in this study, was 1.5% of  
8 Australia's national GHG emissions and is of similar magnitude to emissions associated with  
9 historic savanna deforestation. However, for the deforestation scenario could increase Australia's  
10 GHG emissions by at least 3% per annum for the duration of the expansion, depending on the area  
11 and deforestation rate. These are indicative estimates only, but suggest that the impacts of northern  
12 agricultural development will have an impact on the national GHG budget and will need to be  
13 considered in northern land use decision making processes. These considerations are also  
14 particularly relevant given the emission reduction targets set by Australia following the 21<sup>st</sup>  
15 Conference of Parties to the UN Framework Convention on Climate Change (COP21 / CMP11) to  
16 reduce GHG emissions by 26 to 28% of 2005 by 2030.

17

## 1 **Acknowledgements**

2 Financial support for this study was provided by the Australian Research Council's Linkage  
3 Project LP100100073 and Discovery Project DP0772981. Beringer is funded under the Australian  
4 Research Council's Future Fellowship program (FT1110602). Support for flux data collection and  
5 archiving was provided by Dr Peter Isaac of the Australian flux network, OzFlux  
6 ([www.ozflux.org.au](http://www.ozflux.org.au)), which is funded by the Australian Terrestrial Ecosystem Research Network  
7 (TERN, [www.tern.org.au](http://www.tern.org.au)). Chris and Bridget Schulz provided access to the property and field  
8 assistance throughout all phases of the land use change we monitored. We are grateful for the  
9 technical expertise and field assistance of Matthew Northwood and Michael Brand who maintained  
10 the eddy covariance tower. Yan-Shih Lin, Amanda Lilleyman and Allison O'Keefe provided field  
11 support during the intensive field campaigns. Thanks also to the Department of Environment for  
12 provision of savanna specific deforestation GHG emissions data, 1990-2013 and the two reviewers  
13 who provided constructive comments on the original manuscript.

14

1 **References**

- 2  
3 Adams, V. M. and Pressey, R. L.: Uncertainties around the Implementation of a Clearing-Control  
4 Policy in a unique catchment in Northern Australia: exploring equity issues and balancing  
5 competing objectives, *PLoS One*, 9(5), e9647, 2014.
- 6 Aldrick, J. M., Robinson, C. S.: Report on the Land Units of the Katherine-Douglas Area, Northern  
7 Territory Service, Land Conservation Section of the Northern Territory Administration, Department  
8 of the Interior, Canberra, 1972.
- 9 Anthoni, P. M., Knohl, A., Rebmann, C., Freibauer, A., Mund, M., Ziegler, W., Kolle, O. and  
10 Schulze, E.-D.: Forest and agricultural land-use-dependent CO<sub>2</sub> exchange in Thuringia, Germany,  
11 *Glob. Chang. Biol.*, 10(12), 2005–2019, doi:10.1111/j.1365-2486.2004.00863.x, 2004.
- 12 Aubinet, M., Vesala, T. and Papale, D.: *Eddy Covariance: A Practical Guide to Measurement and*  
13 *Data Analysis*, Springer, Dordrecht., 2012.
- 14 Baccini, A., Goetz, S. J., Walker, W. S., Laporte, N. T., Sun, M., Sulla-Menashe, D., Hackler, J.,  
15 Beck, P. S. A., Dubayah, R., Friedl, M. A., Samanta, S. and Houghton, R. A.: Estimated carbon  
16 dioxide emissions from tropical deforestation improved by carbon-density maps, *Nat. Clim. Chang.*,  
17 2(3), 182–185, 2012.
- 18 Beringer, J., Hutley, L. B., McHugh, I., Arndt, S. K., Campbell, D., Cleugh, H. A., Cleverly, J., de  
19 Dios, V., Eamus, D., Evans, B., Ewenz, C., Grace, P., Griebel, A., Haverd, V., Hinko-Najera, N.,  
20 Huete, A., Isaac, P., Kanniah, K., Leuning, R., Liddell, M. J., Macfarlane, C., Meyer, W., Moore,  
21 C., Pendall, E., Phillips, A., Phillips, R. L., Prober, S., Restrepo-Coupe, N., Rutledge, S., Schroder,  
22 I., Silberstein, R., Southall, P., Sun, M., Tapper, N. J., van Gorsel, E., Vote, C., Walker, J. and  
23 Wardlaw, T.: An introduction to the Australian and New Zealand flux tower network - OzFlux,  
24 *Biogeosciences Discuss.*, 2016, 1–52, doi:10.5194/bg-2016-152, 2016.
- 25 Beringer, J., Hutley, L. B., Tapper, N. J. and Cernusak, L. A.: Savanna fires and their impact on net  
26 ecosystem productivity in North Australia, *Glob. Chang. Biol.*, 13(5), 990–1004,  
27 doi:10.1111/j.1365-2486.2007.01334.x, 2007.
- 28 Beringer, J., Hacker, J., Hutley, L. B., Leuning, R., Arndt, S. K., Amiri, R., Bannehr, L., Cernusak,  
29 L. A., Grover, S., Hensley, C., Hocking, D., Isaac, P., Jamali, H., Kanniah, K., Livesley, S.,  
30 Neining, B., Paw, U. K. T., Sea, W., Straten, D., Tapper, N., Weinmann, R., Wood, S. and  
31 Zegelin, S.: Special-Savanna patterns of energy and carbon integrated across the landscape, *Bull.*  
32 *Am. Meteorol. Soc.*, 92(11), 1467–+, doi:10.1175/2011bams2948.1, 2011.

1 Beringer, J., Hutley, L. B., Abramson, D., Arndt, S. K., Briggs, P., Bristow, M., Canadell, J. G.,  
2 Cernusak, L. A., Eamus, D., Edwards, A. C., Evans, B. J., Fest, B., Goergen, K., Grover, S. P.,  
3 Hacker, J., Haverd, V., Kanniah, K., Livesley, S. J., Lynch, A., Maier, S., Moore, C., Raupach, M.,  
4 Russell-Smith, J., Scheiter, S., Tapper, N. J. and Uotila, P.: Fire in Australian savannas: from leaf to  
5 landscape., *Glob. Chang. Biol.*, 21(1), 62–81, doi:10.1111/gcb.12686, 2015.

6 Beringer, J., McHugh, I., Hutley, L. B., Isaac, P. and Kljun, N.: Dynamic INtegrated Gap-filling  
7 and partitioning for OzFlux (DINGO), *Biogeosciences Discuss*, 1-36, doi:10.5194/bg-2016-188,  
8 2016.

9 Bradshaw, C. J. A.: Little left to lose: deforestation and forest degradation in Australia since  
10 European colonization, *J. Plant Ecol.*, 5(1), 109–120, doi:10.1093/jpe/rtr038, 2012.

11 Brown, S.: Estimating biomass and biomass change of tropical forest: a primer, *FAO Forestry Paper*  
12 134, Rome, [www.fao.org/docrep/w4095e/w4095e00.htm](http://www.fao.org/docrep/w4095e/w4095e00.htm), 1997.

13 Committee on Northern Australia: PIVOT NORTH Inquiry into the Development of Northern  
14 Australia: Final Report, Commonwealth of Australia, Canberra, 2014.

15 Commonwealth of Australia: Australian Vegetation Attribute Manual: National Vegetation  
16 Information System, Version 6.0, Canberra, 2003.

17 Commonwealth of Australia: State and Territory Greenhouse Gas Inventories 2013, Canberra,  
18 2015a.

19 Commonwealth of Australia: Carbon Credits (Carbon Farming Initiative—Emissions Abatement  
20 through Savanna Fire Management) Methodology Determination  
21 ([www.legislation.gov.au/Details/F2015L00344](http://www.legislation.gov.au/Details/F2015L00344)), Department of the Environment, Canberra, 2015b.

22 Cook, G. D.: Historical perspectives on land use development in northern Australia, in *Northern*  
23 *Australia Land and Water Science Review*, Office of North Australia, Commonwealth of Australia,  
24 Canberra, 2009.

25 Eamus, D., Chen, X., Kelley, G. and Hutley, L. B.: Root biomass and root fractal analyses of an  
26 open Eucalyptus forest in a savanna of north Australia, *Aust. J. Bot.*, 50(1), 31–41,  
27 doi:10.1071/bt01054, 2002.

28 Fearnside, P. M., Righi, C. A., Graça, P. M. L. de A., Keizer, E. W. H., Cerri, C. C., Nogueira, E.  
29 M. and Barbosa, R. I.: Biomass and greenhouse-gas emissions from land-use change in Brazil's  
30 Amazonian 'arc of deforestation': The states of Mato Grosso and Rondônia, *For. Ecol. Manage.*,  
31 258(9), 1968–1978, doi:<http://dx.doi.org/10.1016/j.foreco.2009.07.042>, 2009.



1 Ferreira, M. E., Ferreira, L. G., Miziara, F. and Soares-Filho, B. S.: Modeling landscape dynamics  
2 in the central Brazilian savanna biome: future scenarios and perspectives for conservation, *J. Land*  
3 *Use Sci.*, 8(4), 403–421, doi:10.1080/1747423X.2012.675363, 2013.

4 Ferreira, M. E., Ferreira, L. G., Latrubesse, E. M. and Miziara, F.: Considerations about the land use  
5 and conversion trends in the savanna environments of Central Brazil under a geomorphological  
6 perspective, *J. Land Use Sci.*, 11(1), 33–47, 2016.

7 Fisher, R. and Edwards, A. C.: Fire extent and mapping: procedures, validation and website  
8 application, in *Carbon Accounting and Savanna Fire Management*, edited by B. P. Murphy, A. C.  
9 Edwards, C. P. Meyer, and J. Russell-Smith, pp. 57–72, CSIRO Publishing, Melbourne, Australia.,  
10 2015.

11 Fox, I. D., Neldner, V. J., Wilson, G. W. and Bannink, P. J.: *The Vegetation of the Australian*  
12 *Tropical Savannas*, Brisbane, 2001.

13 Galford, G. L., Melillo, J. M., Kicklighter, D. W., Mustard, J. F., Cronin, T. W., Cerri, C. E. P. and  
14 Cerri, C. C.: Historical carbon emissions and uptake from the agricultural frontier of the Brazilian  
15 Amazon, *Ecol. Appl.*, 21(3), 750–763, doi:10.1890/09-1957.1, 2011.

16 Galford, G. L., Soares-Filho, B. and Cerri, C. E. P.: Prospects for land-use sustainability on the  
17 agricultural frontier of the Brazilian Amazon, *Philos. Trans. R. Soc. London B Biol. Sci.*,  
18 368(1619), 2013.

19 Grace, J., San, J. J., Meir, P., Miranda, H. S., Montes, R. A., José, J. S., Meir, P., Miranda, H. S. and  
20 Montes, R. A.: Productivity and carbon fluxes of tropical savannas, *J. Biogeogr.*, 33(3), 387–400,  
21 doi:10.1111/j.1365-2699.2005.01448.x, 2006.

22 Grover, S. P. P., Livesley, S. J., Hutley, L. B., Jamali, H., Fest, B., Beringer, J., Butterbach-Bahl, K.  
23 and Arndt, S. K.: Land use change and the impact on greenhouse gas exchange in north Australian  
24 savanna soils, *Biogeosciences*, 9(1), 423–437, doi:10.5194/bg-9-423-2012, 2012.

25 Grundy, M. J., Bryan, B. A., Nolan, M., Battaglia, M., Hatfield-Dodds, S., Connor, J. D. and  
26 Keating, B. A.: Scenarios for Australian agricultural production and land use to 2050, *Agric. Syst.*,  
27 142, 70–83, doi:10.1016/j.agsy.2015.11.008, 2016.

28 Haverd, V., Raupach, M. R., Briggs, P. R., J. G. Canadell., Davis, S. J., Law, R. M., Meyer, C. P.,  
29 Peters, G. P., Pickett-Heaps, C., and Sherman, B.: The Australian terrestrial carbon budget,  
30 *Biogeosciences*, 10, 851-869, doi:10.5194/bg-10-851-2013, 2013.

31 Henry, B. K., Butler, D. and Wiedemann, S. G.: A life cycle assessment approach to quantifying

1 greenhouse gas emissions from land-use change for beef production in eastern Australia, Rangel. J.,  
2 37 (3), 273–283, doi.org/10.1071/RJ14112, 2015.

3 Houghton, R. A., House, J. I., Pongratz, J., van der Werf, G. R., DeFries, R. S., Hansen, M. C., Le  
4 Quéré, C. and Ramankutty, N.: Carbon emissions from land use and land-cover change,  
5 *Biogeosciences*, 9(12), 5125–5142, doi:10.5194/bg-9-5125-2012, 2012.

6 Hurst, D. F., Griffith, D. W. T. and Cook, G. D.: Trace gas emissions from biomass burning in  
7 tropical Australian savannas, *J. Geophys. Res.*, 99(D8), 16441, doi:10.1029/94JD00670, 1994.

8 Hutley, L. B. and Beringer, J.: Disturbance and climatic drivers of carbon dynamics of a north  
9 Australian tropical savanna, in *Ecosystem Function in Savannas: Measurement and Modeling at  
10 Landscape to Global*, edited by M. J. Hill and N. P. Hanan, CRC Press, Boca Raton., 2011.

11 Hutley, L. B., Leuning, R., Beringer, J. and Cleugh, H. A.: The utility of the eddy covariance  
12 techniques as a tool in carbon accounting: tropical savanna as a case study, *Aust. J. Bot.*, 53(7),  
13 663–675, doi:10.1071/bt04147, 2005.

14 Hutley, L. B., Beringer, J., Isaac, P. R., Hacker, J. M. and Cernusak, L. A.: A sub-continental scale  
15 living laboratory: Spatial patterns of savanna vegetation over a precipitation gradient in northern  
16 Australia, *Agric. For. Meteorol.*, 151(11), 1417–1428, doi:10.1016/j.agrformet.2011.03.002, 2011.

17 IPCC: Revised 1996 Intergovernmental Panel on Climate Change (IPCC) Guidelines for National  
18 Greenhouse Gas Inventories 3 vols, IPCC/OECD/IEA: Paris, France, 1997.

19 IPCC: Guidelines for National Greenhouse Gas Inventories, Paris., 2003.

20 IPCC: Climate Change 2013: The Physical Science Basis. Contribution of Working Group I to the  
21 Fifth Assessment Report of the Intergovernmental Panel on Climate Change. Eds. Stocker, T.F., D.  
22 Qin, G.-K. Plattner, M. Tignor, S.K. Allen, J. Boschung, A. Nauels, Y. Xia, V. Bex and P.M.  
23 Midgley, Cambridge University Press: Cambridge, United Kingdom, 2013

24 Isaac, P., Cleverly, J., McHugh, I., van Gorsel, E., Ewenz, C. and Beringer, J.: OzFlux Data:  
25 network integration from collection to curation, *Biogeosciences Discuss.*, 2016, 1–41,  
26 doi:10.5194/bg-2016-189, 2016..

27 Isbell, R.: The Australian Soil Classification. In: *Australian Soil and Land Survey Handbook*,  
28 CSIRO Publishing, Melbourne, 2002.

29 Jamali, H., Livesley, S. J., Dawes, T. Z., Hutley, L. B. and Arndt, S. K.: Termite mound emissions  
30 of CH<sub>4</sub> and CO<sub>2</sub> are primarily determined by seasonal changes in termite biomass and behaviour,  
31 *Oecologia*, 167(2), 525–534, doi:10.1007/s00442-011-1991-3, 2011a.

- 1 Jamali, H., Livesley, S. J., Grover, S. P., Dawes, T. Z., Hutley, L. B., Cook, G. D. and Arndt, S. K.:  
2 The Importance of Termites to the CH<sub>4</sub> Balance of a Tropical Savanna Woodland of Northern  
3 Australia, *Ecosystems*, 14(5), 698–709, doi:10.1007/s10021-011-9439-5, 2011b.
- 4 Jarecki, M. K. and Lal, R.: Crop Management for Soil Carbon Sequestration, *Cr. Rev. Plant Sci.*,  
5 22, 471–502, doi:10.1080/07352680390253179, 2003.
- 6 Johnson, A.: North Australian Grassland Fuel Guide – Sturt Plateau and Victoria River District,  
7 Cooperative Research Centre for Tropical Savannas Management, Charles Darwin University,  
8 Darwin, Australia, 2001.
- 9 Jones, D., Wang, W. and Fawcett, R.: High-quality spatial climate data sets for Australia, *Aust.*  
10 *Meteorol. Oceanogr. J.*, 58, 233–248, 2009.
- 11 Lal, R. and Follett, R. F.: Soils and climate change, in *Soil Carbon Sequestration and the*  
12 *Greenhouse Effect*, edited by R. Lal and R. F. Follett, pp. 1–23, Soil Science Society of America,  
13 Maddison., 2009.
- 14 Lambin, E. F., Gibbs, H. K., Ferreira, L., Grau, R., Mayaux, P., Meyfroidt, P., Morton, D. C., Rudel,  
15 T. K., Gasparri, I. and Munger, J.: Estimating the world’s potentially available cropland using a  
16 bottom-up approach, *Glob. Environ. Chang.*, 23(5), 892–901, doi:10.1016/j.gloenvcha.2013.05.005,  
17 2013.
- 18 Landsberg, J., Gillieson, D. and Salt, D.: *Trees in savanna landscapes: finding the balance*, David  
19 Gillison, Cooperative Research Centre for Tropical Savannas Management, Charles Darwin  
20 University, Darwin, Australia, 2011.
- 21 Lapola, D. M., Martinelli, L. A., Peres, C. A., Ometto, J. P. H. B., Ferreira, M. E., Nobre, C. A.,  
22 Aguiar, A. P. D., Bustamante, M. M. C., Cardoso, M. F., Costa, M. H., Joly, C. A., Leite, C. C.,  
23 Moutinho, P., Sampaio, G., Strassburg, B. B. N. and Vieira, I. C. G.: Pervasive transition of the  
24 Brazilian land-use system, *Nat. Clim. Chang.*, 4(1), 27–35, doi.org/10.1038/nclimate2056, 2014.
- 25 Law, R. and Garnett, S. T.: Understanding carbon in the Northern Territory: an analysis of future  
26 land use scenarios using the national carbon accounting tool, Cooperative Research Centre for  
27 Tropical Savannas Management, Darwin, 2009.
- 28 Law, R. and Garnett, S. T.: Mapping carbon in tropical Australia: Estimates of carbon stocks and  
29 fluxes in the Northern Territory using the national carbon accounting toolbox, *Ecol. Manag. Restor.*,  
30 12(1), 61–68, doi:10.1111/j.1442-8903.2011.00566.x, 2011.
- 31 Lawes, M. J., Greiner, R., Leiper, I. A., Ninnis, R., Pearson, D. and Boggs, G.: The effects of a

1 moratorium on land-clearing in the Douglas-Daly region, Northern Territory, Australia, *Rangel. J.*,  
2 37(4), 399–408, doi.org/10.1071/RJ15014, 2015.

3 Le Quéré, C., Moriarty, R., Andrew, R. M., Peters, G. P., Ciais, P., Friedlingstein, P., Jones, S. D.,  
4 Sitch, S., Tans, P., Arneeth, A., Boden, T. A., Bopp, L., Bozec, Y., Canadell, J. G., Chini, L. P.,  
5 Chevallier, F., Cosca, C. E., Harris, I., Hoppema, M., Houghton, R. A., House, J. I., Jain, A. K.,  
6 Johannessen, T., Kato, E., Keeling, R. F., Kitidis, V., Klein Goldewijk, K., Koven, C., Landa, C. S.,  
7 Landschützer, P., Lenton, A., Lima, I. D., Marland, G., Mathis, J. T., Metzl, N., Nojiri, Y., Olsen,  
8 A., Ono, T., Peng, S., Peters, W., Pfeil, B., Poulter, B., Raupach, M. R., Regnier, P., Rödenbeck, C.,  
9 Saito, S., Salisbury, J. E., Schuster, U., Schwinger, J., Séférian, R., Segsneider, J., Steinhoff, T.,  
10 Stocker, B. D., Sutton, A. J., Takahashi, T., Tilbrook, B., van der Werf, G. R., Viovy, N., Wang, Y.-  
11 P., Wanninkhof, R., Wiltshire, A. and Zeng, N.: Global carbon budget 2014, *Earth Syst. Sci. Data*,  
12 7(1), 47–85, doi:10.5194/essd-7-47-2015, 2015.

13 Macfarlane, C., Hoffman, M., Eamus, D., Kerp, N., Higginson, S., McMurtrie, R. and Adams, M.:  
14 Estimation of leaf area index in eucalypt forest using digital photography, *Agric. For. Meteorol.*,  
15 143(3–4), 176–188, doi:10.1016/j.agrformet.2006.10.013, 2007.

16 Mayocchi, C. L. and Bristow, K. L.: Soil surface heat flux: some general questions and comments  
17 on measurements, *Agric. For. Meteorol.*, 75, 43–50, 1995.

18 Meyer, C. P., Cook, G. D., Reisen, F., Smith, T. E. L., Tattaris, M., Russell-Smith, J., Maier, S. W.,  
19 Yates, C. P. and Wooster, M. J.: Direct measurements of the seasonality of emission factors from  
20 savanna fires in northern Australia, *J. Geophys. Res. Atmos.*, 117(D20), n/a-n/a,  
21 doi:10.1029/2012JD017671, 2012.

22 Murphy, B. P., Lehmann, C. E. R., Russell-Smith, J. and Lawes, M. J.: Fire regimes and woody  
23 biomass dynamics in Australian savannas, *J. Biogeogr.*, 41(1), 133–144, doi:10.1111/jbi.12204,  
24 2014.

25 Murphy, B. P., Edwards, A. C., Meyer, C. P. (Mick) and Russell-Smith, J.: *Carbon Accounting and*  
26 *Savanna Fire Management*, CSIRO Publishing, Melbourne, 2015a.

27 Murphy, B. P., Liedloff, A. C. and Cook, G. D.: Does fire limit tree biomass in Australian  
28 savannas? *Int. J. Wildl. Fire*, 24(1), 1, doi:10.1071/WF14092, 2015b.

29 Neill, C., Piccolo, M. C., Cerri, C. C., Steudler, P. a. and Melillo, J. M.: Soil solution nitrogen  
30 losses during clearing of lowland Amazon forest for pasture, *Plant Soil*, 281(1–2), 233–245,  
31 doi:10.1007/s11104-005-4435-1, 2006.

32 Petheram, C., McMahon, T. A. and Peel, M. C.: Flow characteristics of rivers in northern Australia:

1 Implications for development, *J. Hydrol.*, 357(1-2), 93–111, doi:10.1016/j.jhydrol.2008.05.008,  
2 2008.

3 Petheram, C., McMahon, T. A., Peel, M. C. and Smith, C. J.: A continental scale assessment of  
4 Australia's potential for irrigation, *Water Resour. Manag.*, 24(9), 1791–1817, doi:10.1007/s11269-  
5 009-9525-z, 2009.

6 Petheram, C., Gallant, J., Wilson, P., Stone, P., Eades, G., Roger, L., Read, A., Tickell, S.,  
7 Commander, P., Moon, A., McFarlane, D. and Marvanek, S. .: Northern rivers and dams: a  
8 preliminary assessment of surface water storage potential for northern Australia, Canberra, 2014.

9 Reichstein, M., Falge, E., Baldocchi, D., Papale, D., Aubinet, M., Berbigier, P., Bernhofer, C.,  
10 Buchmann, N., Gilmanov, T., Granier, A., Grunwald, T., Havrankova, K., Ilvesniemi, H., Janous,  
11 D., Knohl, A., Laurila, T., Lohila, A., Loustau, D., Matteucci, G., Meyers, T., Miglietta, F.,  
12 Ourcival, J.-M., Pumpanen, J., Rambal, S., Rotenberg, E., Sanz, M., Tenhunen, J., Seufert, G.,  
13 Vaccari, F., Vesala, T., Yakir, D. and Valentini, R.: On the separation of net ecosystem exchange  
14 into assimilation and ecosystem respiration: review and improved algorithm, *Glob. Chang. Biol.*,  
15 11(9), 1424–1439, doi:10.1111/j.1365-2486.2005.001002.x, 2005.

16 Richards, G. P. and Evans, D. M. W.: Development of a carbon accounting model (FullCAM Vers.  
17 1.0) for the Australian continent, *Aust. For.*, 67, 277–283, doi:10.1080/00049158.2004.10674947,  
18 2004.

19 Rose, D.: The dynamics of coarse woody debris in the mesic tropical savannas of the Darwin  
20 region: abundance, decomposition and consumption by fire, Honours Thesis, Charles Darwin  
21 University, 2006.

22 Russell-Smith, J., Whitehead, P. J., Cooke, P. M. and Yates, C. P.: Challenges and opportunities for  
23 fire management in fire-prone northern Australia, in *Culture, Ecology and Economy of Fire*  
24 *Management in North Australian Savannas*, edited by J. Russell-Smith, P. J. Whitehead, and P. M.  
25 Cooke, pp. 1–23, CSIRO Publishing, Melbourne, 2009a.

26 Russell-Smith, J., Murphy, B. P., Meyer, C. P. (Mick), Cook, G. D., Maier, S., Edwards, A. C.,  
27 Schatz, J. and Brocklehurst, P.: Improving estimates of savanna burning emissions for greenhouse  
28 accounting in northern Australia: limitations, challenges, applications, *Int. J. Wildl. Fire*, 18(1), 1,  
29 doi:10.1071/WF08009, 2009b.

30 Russell-Smith, J., Cook, G. D., Cooke, P. M., Edwards, A. C., Lendrum, M., Meyer, C. P. (Mick)  
31 and Whitehead, P. J.: Managing fire regimes in north Australian savannas: applying Aboriginal  
32 approaches to contemporary global problems, *Front. Ecol. Environ.*, 11(s1), e55–e63,

1 doi:10.1890/120251, 2013.

2 Sakai, R. K., Fitzjarrald, D. R., Moraes, O. L. L., Staebler, R. M., Acevedo, O. C., Czikowsky, M.  
3 J., da Silva, R., Braitt, E. and Miranda, V.: Land-use change effects on local energy, water, and  
4 carbon balances in an Amazonian agricultural field., *Glob. Chang. Biol.*, 10(5), 895–907,  
5 doi:10.1111/j.1529-8817.2003.00773.x, 2004.

6 Sanderman, J., Farquharson, R. and Baldock, J. A.: Soil carbon sequestration potential: a review for  
7 Australian agriculture. Report to the Australian Department of Climate Change, Adelaide, 2010.

8 Steffan, W. and Hughes, L.: The Critical Decade 2013: Climate change science, risks and response,  
9 Climate Commission Secretariat, Department of Industry, Innovation, Climate Change, Science,  
10 Research and Tertiary Education, Canberra, 2013.

11 Surawski, N. C., Sullivan, A. L., Roxburgh, S. H. and Cook, G. D.: Review of FullCAM forest fire  
12 event parameters with recommendations supported by a literature review, CSIRO Ecosystems  
13 Science, Canberra, 2012.

14 Thackway, R.A.: A vegetation fuel type map for Australia's northern savannas, Department of the  
15 Environment, Canberra, 2014.

16 Tian, H., Chen, G., Lu, C., Xu, X., Ren, W., Zhang, B., Banger, K., Tao, B., Pan, S., Liu, M.,  
17 Zhang, C., Bruhwiler, L. and Wofsy, S.: Global methane and nitrous oxide emissions from  
18 terrestrial ecosystems due to multiple environmental changes, *Ecosyst. Heal. Sustain.*, 1(1), art4,  
19 doi:10.1890/EHS14-0015.1, 2015.

20 Tubiello, F. N., Salvatore, M., Ferrara, A. F., House, J., Federici, S., Rossi, S., Biancalani, R.,  
21 Condor Golec, R. D., Jacobs, H., Flammini, A., Prosperi, P., Cardenas-Galindo, P., Schmidhuber,  
22 J., Sanz Sanchez, M. J., Srivastava, N. and Smith, P.: The contribution of agriculture, forestry and  
23 other land use activities to global warming, 1990–2012, *Glob. Chang. Biol.*, 21(7), 2655–2660,  
24 doi:10.1111/gcb.12865, 2015.

25 van der Werf, G. R., Randerson, J. T., Giglio, L., Collatz, G. J., Mu, M., Kasibhatla, P. S., Morton,  
26 D. C., DeFries, R. S., Jin, Y. and van Leeuwen, T. T.: Global fire emissions and the contribution of  
27 deforestation, savanna, forest, agricultural, and peat fires (1997–2009), *Atmos. Chem. Phys.*,  
28 10(23), 11707–11735, doi:10.5194/acp-10-11707-2010, 2010.

29 Walsh, D., Russell-Smith, J. and Cowley, R.: Fire and carbon management in a diversified  
30 rangelands economy: research, policy and implementation challenges for northern Australia,  
31 *Rangel. J.*, 36(4), 313–322, doi:http://dx.doi.org/10.1071/RJ13122, 2014.

- 1 Weitz, A. M., Veldkamp, E., Keller, M., Neff, J. and Crill, P. M.: Nitrous oxide, nitric oxide, and  
2 methane fluxes from soils following clearing and burning of tropical secondary forest, *J. Geophys.*  
3 *Res.*, 103(D21), 28047, doi:10.1029/98JD02144, 1998.
- 4 Whitehead, P. J., Russell-Smith, J. and Yates, C.: Fire patterns in north Australian savannas:  
5 extending the reach of incentives for savanna fire emissions abatement, *Rangel. J.*, 36(4), 371–388,  
6 2014.
- 7 Williams, R. J., Zerihun, A., Montagu, K. D., Hoffman, M., Hutley, L. B. and Chen, X.: Allometry  
8 for estimating aboveground tree biomass in tropical and subtropical eucalypt woodlands: towards  
9 general predictive equations, *Aust. J. Bot.*, 53(7), 607, doi:10.1071/BT04149, 2005.
- 10 Woinarski, J., Mackey, B., Nix, H. and Traill, B.: The nature of Northern Australia: it's natural  
11 values, ecological processes and future prospects, ANU E Press, Canberra., 2007.
- 12 Woldendorp, G., Keenan, R. J., Barry, S. and Spenser, R. D.: Analysis of sampling methods for  
13 coarse woody debris, *For. Ecol. Manage.*, 198, 133–148, 2004.
- 14 Wolf, S., Eugster, W., Potvin, C. and Buchmann, N.: Strong seasonal variations in net ecosystem  
15 CO<sub>2</sub> exchange of a tropical pasture and afforestation in Panama, *Agric. For. Meteorol.*, 151(8),  
16 1139–1151, doi:10.1016/j.agrformet.2011.04.002, 2011.
- 17 Zenone, T., Chen, J., Deal, M. W., Wilske, B., Jasrotia, P., Xu, J., Bhardwaj, A. K., Hamilton, S. K.  
18 and Philip Robertson, G.: CO<sub>2</sub> fluxes of transitional bioenergy crops: effect of land conversion  
19 during the first year of cultivation, *GCB Bioenergy*, 3(5), 401–412, doi:10.1111/j.1757-  
20 1707.2011.01098.x, 2011.
- 21 Zona, D., Janssens, I. A., Aubinet, M., Gioli, B., Vicca, S., Fichot, R. and Ceulemans, R.: Fluxes of  
22 the greenhouse gases (CO<sub>2</sub>, CH<sub>4</sub> and N<sub>2</sub>O) above a short-rotation poplar plantation after  
23 conversion from agricultural land, *Agric. For. Meteorol.*, 169, 100–110, 2013.

24

1 **Table captions**

2

3 Table 1 Site characteristics for the uncleared savanna (UC) and cleared (CS) sites. Site soil orders  
4 are given as per Isbell (2002) with savanna vegetation classified using Fox et al. (2001). Fire  
5 frequency was estimated from fire mapping taken from the North Australian Fire Information  
6 system (NAFI, [www.firenorth.org.au](http://www.firenorth.org.au)) for 2000-2012. The fire frequency estimate for the CS site  
7 excluded the debris fires in August 2012. Basal area and stem density is provided for all woody  
8 stems >2 cm DBH at both sites. Mean site LAI for the UC is taken from Hutley et al. 2011 and for  
9 the CS site, was estimated from canopy hemispherical photos, see text for details.

10 Table 2 Characteristics of land conversion phases during the 668 day observation period at the  
11 savanna clearing site (CS). Also given are the canopy heights following LUC phases and flux  
12 instrument heights that were adjusted following clearing, burning and then soil preparation phases.

13 Table 3 Cumulative precipitation and mean NEE, Re and GPP ( $\text{Mg C ha}^{-1} \text{ month}^{-1}$ ) for each of the  
14 LUC phases at the CS site as measured by the flux tower. These fluxes are given for the UC site for  
15 these same periods. One-way ANOVA was used to test for differences between mean daily NEE for  
16 each LUC phase with significantly different means labelled with an asterisk. On the days of ignition  
17 during the debris burning phase, flux data at the CS site were excluded. Integrated fluxes are given  
18 for the post-clearing period (507 days) and the entire observation period (668 days) for both sites in  
19  $\text{Mg C ha}^{-1}$ .

20 Table 4 Measured fuel loads, assumed burning efficiencies (BEF), carbon contents, N:C ratio and  
21 emissions factors (EF) used to estimate GHG emissions from the burning of the post-deforestation  
22 fine, coarse and heavy fuel debris. Emission factors, carbon content and C:N ratio were assumed for  
23 the vegetation fuel type woodland savanna with mixed grass (code hWMI) as given in the  
24 Emissions Abatement through Savanna Fire Management methodology (Commonwealth of  
25 Australia, 2015b), available at [www.legislation.gov.au/Details/F2015L00344](http://www.legislation.gov.au/Details/F2015L00344) and Meyers et al.  
26 2012.

27 Table 5 Greenhouse gas emissions for 1990-2013 from prescribed savanna burning and savanna  
28 deforestation at catchment (Douglas-Daly River), state/territory (Northern Territory savanna area)  
29 and regional scales (north Australian savanna area, Fig. 1). For savanna burning, burnt area and  
30 associated mean annual emissions ( $\pm$  SD) are given for both reportable non-CO<sub>2</sub> (CH<sub>4</sub>, N<sub>2</sub>O) and  
31 total emissions (CO<sub>2</sub>, CH<sub>4</sub> and N<sub>2</sub>O). For the identical areas as used for savanna burning, mean  
32 annual GHG emissions from deforestation ( $\pm$  SD) are given. For the Douglas-Daly River



1 catchment, deforestation area was taken from Lawes et al. (2015) and combined with deforestation  
2 emissions from the CS site. Deforestation emissions (1990-2013) for the NT and the north  
3 Australian savanna area are taken from the State and Territory Greenhouse Gas Inventories  
4 (Commonwealth of Australia, 2015a). In bold text are the emissions associated with the current  
5 deforestation rate plus expanded deforestation areas as identified by Petheram et al. (2014), which  
6 are combined with emissions from the CS site to give an upscaled estimate of potential emissions  
7 with agricultural development at the three spatial scales.

8

9 Table 1

10

<i>Site</i>	<i>UC</i>	<i>CS</i>
Location	14°09'33.12"S, 131°23'17.16"E	14°33'48.71"S, 132°28'39.47"E
Soils	Red Kandosol	Red Kandosol
Vegetation type	Savanna woodland with mixed grasses Map unit <b>D4</b> . <i>E. tetradonta</i> , <i>C. latifolia</i> , <i>Terminalia grandiflora</i> , <i>Sorghum spp</i> , <i>Heteropogon triticeus</i>	Savanna woodland with mixed grasses Map unit <b>D4</b> . <i>E. tetradonta</i> , <i>Erythrophleum chlorostachys</i> , <i>Corymbia. bleeseri</i> , <i>Sorghum spp</i> , <i>H. triticeus</i>
Map unit area (km <sup>2</sup> )	59,986	59,986
Fire frequency (y <sup>-1</sup> )	0.23	0.07
Basal area (m <sup>2</sup> ha <sup>-1</sup> )	8.3	6.8
Canopy height (m)	16.4	14.2
Above-ground biomass (Mg C ha <sup>-1</sup> )	30.6 ± 9.2	26.2 ± 7.0
Stem density (ha <sup>-1</sup> )	330 ± 58	643 ± 102
Overstorey LAI (wet/dry)	n/a / 0.8	0.9 / 0.5
MODIS LAI (wet/dry)	1.5 / 0.9	1.6 / 1.0
MAP (mm)	1372 <sup>a</sup> / 1180 <sup>b</sup>	1107 <sup>c</sup>
Max T <sub>air</sub> (°C)	37.5 (Oct) / 31.2 (Jun)	37.5 (Oct) / 29.7 (Jun)
Min T <sub>air</sub> (°C)	23.8 (Jan) / 12.6 (Jul)	25.0 (Nov) / 13.7 (Jul)

11 <sup>a</sup>On-site observations, 2007-2012, <sup>b</sup>gridded precipitation (AWAP, 1970-2012), <sup>c</sup>Tindal BoM station (14.52S, 132.38E, data from 1985-2013).

12

13

14 Table 2  
 15  
 16

<i>Season</i>	<i>Period</i>	<i>LULUC phases</i>	<i>Canopy height (m)</i>	<i>Instrument height (m)</i>
Late dry season	Sep - Oct 2011	Intact savanna	16	21.5
Wet season pre-clearing	Oct 2011 - Feb 2012	Intact savanna	16	21.5
Wet season clearing	Mar - May 2012	Savanna deforested using bulldozers, followed by debris decomposition, understory grass germination	3	7
Dry season pre- burn	May - Aug 2012	Vegetation debris curing, understorey grass growth	2	7
Debris burning	Aug 2012	Debris and grasses burnt, soil ripped to 60 cm to remove roots, roots and remaining debris stockpiled, re-burnt	2	7
Dry season post-burn	Aug - Nov 2012	Grass and shrubs germination and resprouting	1	7
Early wet season	Nov 2012 - Jan 2013	Removal remaining below-ground biomass. Wet season rains stimulates grass growth, shrub re-sprouting and growth	1	7
Wet season	Jan - Mar 2013	All regenerated vegetation removed, soil bed preparation	0	3
Dry season	Apr - Jul 2013	Soil cultivation in stages	0	3

17

18

19 Table 3  
 20  
 21

<i>LULUC phases</i>	<i>Phase number</i>	<i>Period (d)</i>	<i>CS</i>				<i>UC</i>			
			<i>Rainfall (mm)</i>	<i>NEE (Mg C ha<sup>-1</sup> month<sup>-1</sup>)</i>	<i>Re</i>	<i>GPP</i>	<i>Rainfall (mm)</i>	<i>NEE (Mg C ha<sup>-1</sup> month<sup>-1</sup>)</i>	<i>Re</i>	<i>GPP</i>
Intact canopy cover	1	161	736.6	-0.23	1.57	-1.79	1076.8	-0.25	1.45	-1.70
Clearing event	2	4	59.4	0.23*	1.95	-1.73	59.8	0.38*	1.80	-1.50
Wet-dry debris curing, decomposition	3	59	143.2	0.98**	1.39	-0.41	412.0	0.32**	1.53	-1.22
Dry season pre-burn	4	94	0	0.34**	0.57	-0.23	2.4	0.15**	0.94	-0.79
Fire emissions late dry	5	22	0	0.90**	0.76	0.0	0.0	-0.01**	0.71	-0.72
Dry season post-burn	6	67	2.2	0.31**	0.37	-0.06	64.4	-0.28	0.64	-0.91
Early wet regrowth	7	80	361.0	0.03**	0.99	-0.96	345.8	-0.32	1.80	-2.12
Wet season site prep	8	91	701.7	0.62**	0.99	-0.37	914.4	-0.20**	1.67	-1.88
Dry season final bed prep. and cultivation	9	90	0	0.29**	0.32	-0.02	10.8	0.06**	0.91	-0.85
				<i>(Mg C ha<sup>-1</sup>)</i>				<i>(Mg C ha<sup>-1</sup>)</i>		
Total post-clearing		507	1267.5	7.2**	12.8	-5.6	1809.6	-0.78**	20.7	-21.5
Total all phases		668	2004.1	6.0**	21.2	-15.2	2886.4	-2.1**	28.5	-30.6

22 \*Denotes significantly different mean NEE at the 5% level, \*\* significant at 1%.  
 23

24 Table 4

25

<i>Fuel type</i>	<i>Fuel load (Mg C ha<sup>-1</sup>)</i>	<i>BEF</i>	<i>Carbon content</i>	<i>N:C ratio</i>	<i>EF CO<sub>2</sub></i>	<i>EF CH<sub>4</sub></i>	<i>EF N<sub>2</sub>O</i>	<i>Emissions (Mg CO<sub>2</sub>-e ha<sup>-1</sup>)</i>			
								<i>CO<sub>2</sub></i>	<i>CH<sub>4</sub></i>	<i>N<sub>2</sub>O</i>	<i>Total</i>
Fine	1.1 ± 0.70	0.95	0.46	0.0096	0.97	0.0031	0.0075	3.9	0.1	0.04	4.0
Coarse	0.5 ± 1.0	0.9	0.46	0.0081	0.92	0.0031	0.0075	1.5	0.0	0.01	1.6
Heavy - AGB	26.2 ± 7.0	0.9	0.46	0.0081	0.87	0.01	0.0036	75.2	7.9	0.32	83.4
Heavy - CWD	1.4 ± 0.6	0.9	0.46	0.0081	0.87	0.01	0.0036	4.0	2.7	0.11	28.5
Heavy - BGB	9.0 ± 2.4	0.9	0.46	0.0081	0.87	0.01	0.0036	25.7	0.0	0.02	4.4
<i>Total</i>								<i>110.2</i>	<i>11.1</i>	<i>0.50</i>	<i>121.9</i>

26

27

28 Table 5  
 29  
 30

<i>Savanna region</i>	<i>Savanna burning</i>			<i>Savanna deforestation</i>			
	Burnt area <sup>a</sup> (ha y <sup>-1</sup> )	Emissions non-CO <sub>2</sub> <sup>a</sup> (Gg CO <sub>2</sub> -e y <sup>-1</sup> )	Emissions total <sup>a</sup> (Gg CO <sub>2</sub> -e y <sup>-1</sup> )	Deforestation area (ha y <sup>-1</sup> )	Emissions total (Gg CO <sub>2</sub> -e y <sup>-1</sup> )	Expanded deforestation area <sup>d</sup> (ha)	Expanded emissions total <sup>d</sup> (Gg CO <sub>2</sub> -e y <sup>-1</sup> )
Douglas-Daly River catchment	2,482,100 ±490,400	577 ±124	14,270 ±3064	1275 ±454 <sup>b</sup>	163 ±162 <sup>b</sup>	<b>20,000</b>	<b>756</b>
Northern Territory	13,419,410 ±487,300	3,490 ±922	86,255 ±22,880	1,717 ±611 <sup>c</sup>	398 ±128 <sup>c</sup>	<b>114,500</b>	<b>3,413</b>
North Australian	32,249,254 ±11,176,004	6,740 ±1,729	166,586 ±42,725	78,605 ±34,976 <sup>c</sup>	16,161 ±5601 <sup>c</sup>	<b>311,000</b>	<b>24,393</b>

31 <sup>a</sup>Burnt area and emissions data estimated using the on-line Savanna Burning Abatement Tool (SAVBat2), 1990-2013. These emissions are CH<sub>4</sub> and N<sub>2</sub>O only.

32 <sup>b</sup>Deforestation area data taken from Lawes et al. (2015), upscaled using the emissions from the CS site from this study, 1990-2013

33 <sup>c</sup>Deforestation area and emissions data taken from the State and Territory Greenhouse Gas Inventories (Commonwealth of Australia, 2015a), 1990-2013

34 <sup>d</sup>Expanded deforestation area data taken from catchments as identified by Petheram et al. (2014), upscaled using the GHG emissions from the CS site from this study and added  
 35 to historic emissions

36

37 **Figure captions**

38

39 Figure 1 Location of the uncleared site (UC) and the cleared savanna (CS) sites south of Darwin,  
40 Northern Territory. The inset figure shows the distribution of the savanna biome across northern  
41 Australia as defined by Fox et al. (2001).

42 Figure 2 Comparative meteorology and fluxes for the uncleared (UC) and cleared savanna CS sites  
43 prior to the clearing event. Data spans the late dry season (September 2011) through to the mid-wet  
44 season prior to the clearing event of 2-6 March 2012. Plots include a) daily precipitation (black bars  
45 UC site, grey bars CS site), mean daily  $T_{\text{air}}$  (black lines UC, grey CS), b) mean daily VPD (dashed  
46 lines; black UC, grey CS), c) interpolated 8-day MODIS LAI (black UC, grey CS), d) NEE (black  
47 UC, grey CS) partitioned into  $R_e$  (red UC, pink CS) and GPP (dark green UC, pale green CS).

48 Figure 3a) Daily precipitation and b) diurnal patterns of NEE at the CS site for the week prior to the  
49 clearing event of 2-6 March 2012 (vertical bar) and three weeks post-clearing.

50 Figure 4 Cumulative NEE from the CS (red line) and UC sites (black line) for each land use phase  
51 (see Table 2 for details) over the entire observational period, September 2011 to July 2013. The UC  
52 site is a long-term savanna site of the Australian flux network (OzFlux, see Beringer et al. 2016a)  
53 and using the sites' 8-year flux record (2007-2013), the long-term cumulative mean NEE is plotted  
54 for each land use phase of (grey line;  $\pm$  95% CI). The dashed line indicates zero net  $\text{CO}_2$  flux.

55

56 **Plate caption**  
57

58 Plate 1 Key LUC phases associated with: a) the clearing event, Phase 3; b) debris burning of the  
59 cured grass, litter and woody fuels following the 5 month curing period, Phase 5; c) stockpiling and  
60 ignition of remaining unburnt debris and d) post-fire site preparation with all biomass consumed,  
61 Phase 9.

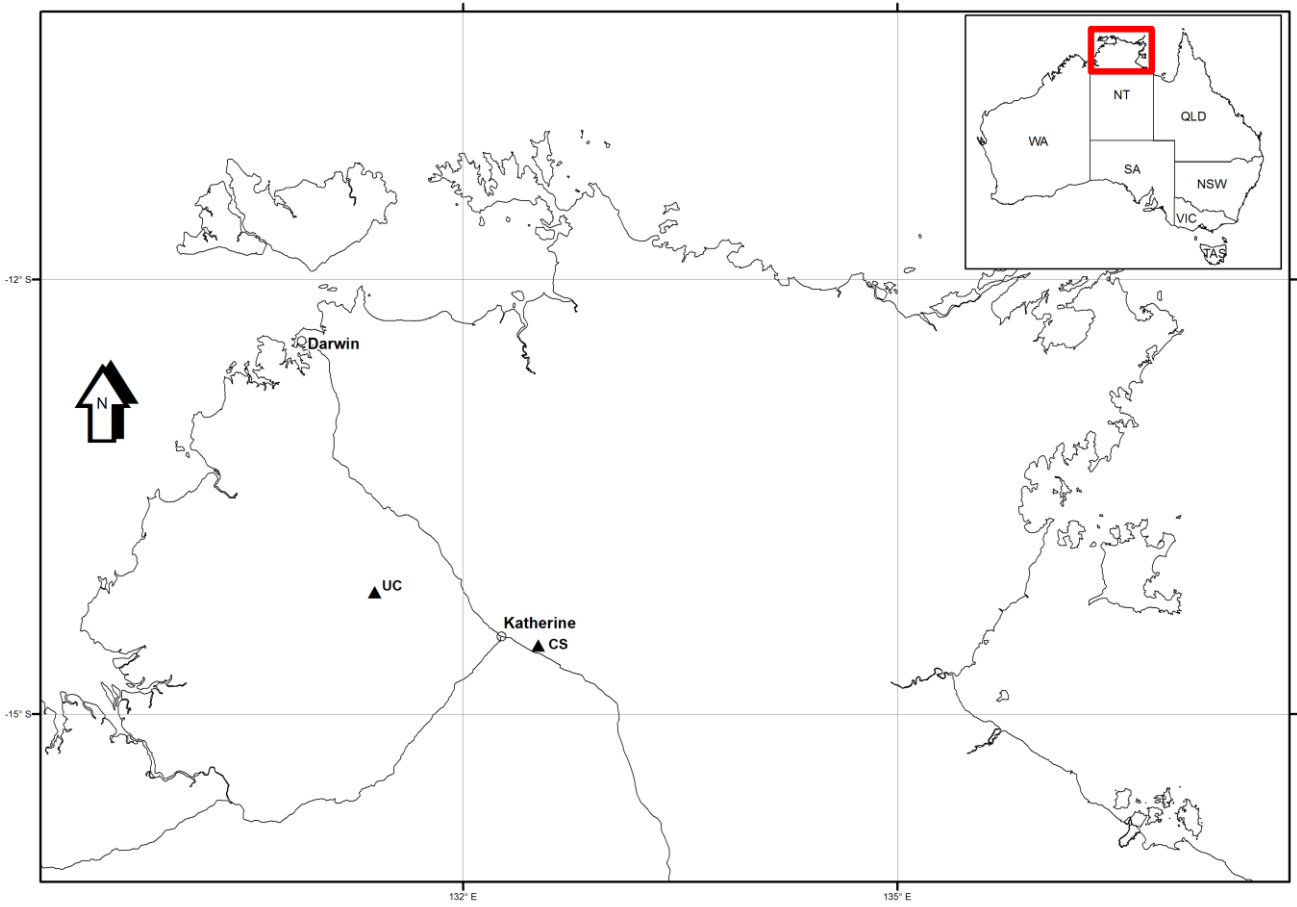
62

63

64



65 Figure 1

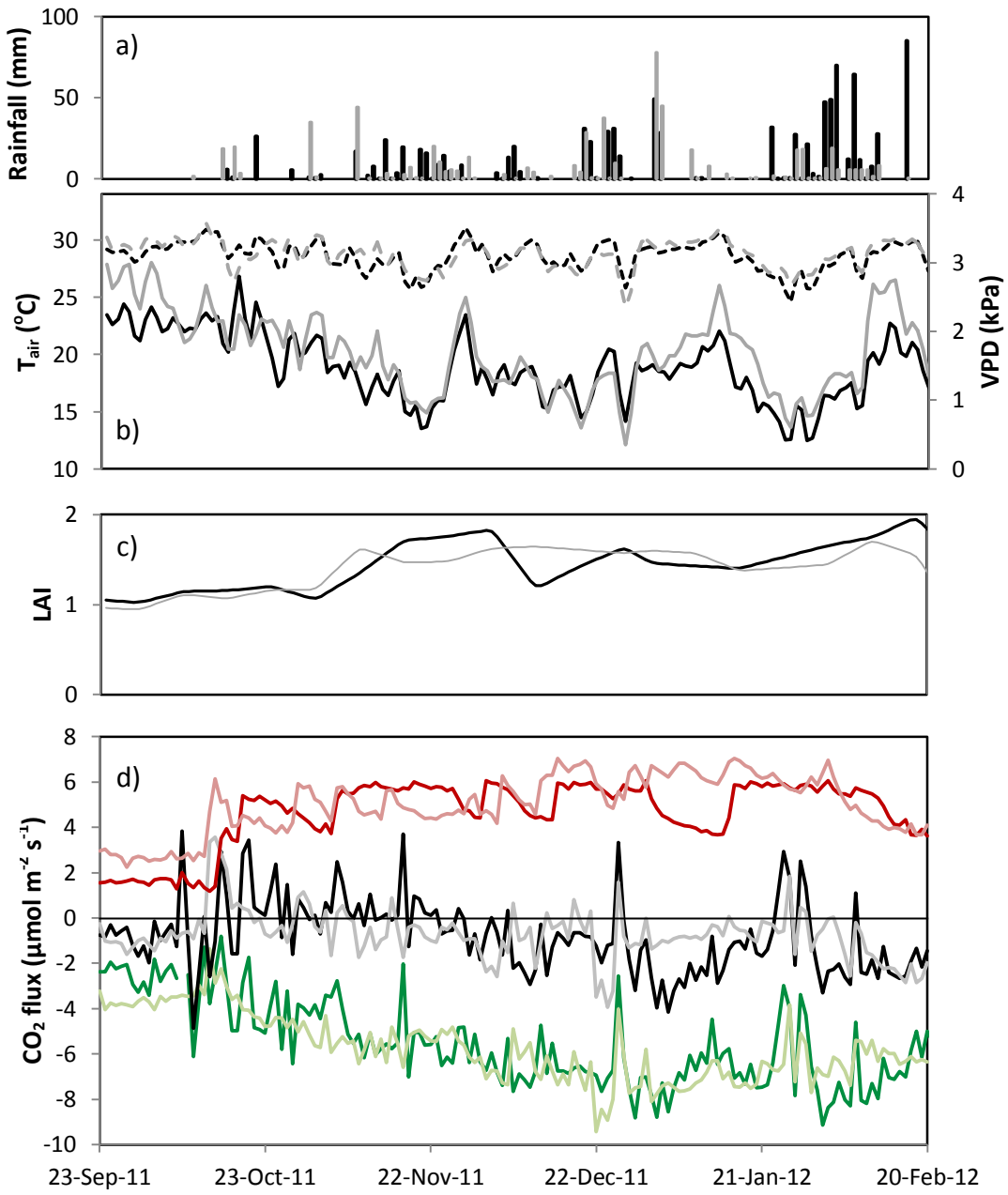


66

67

68 Figure 2

69

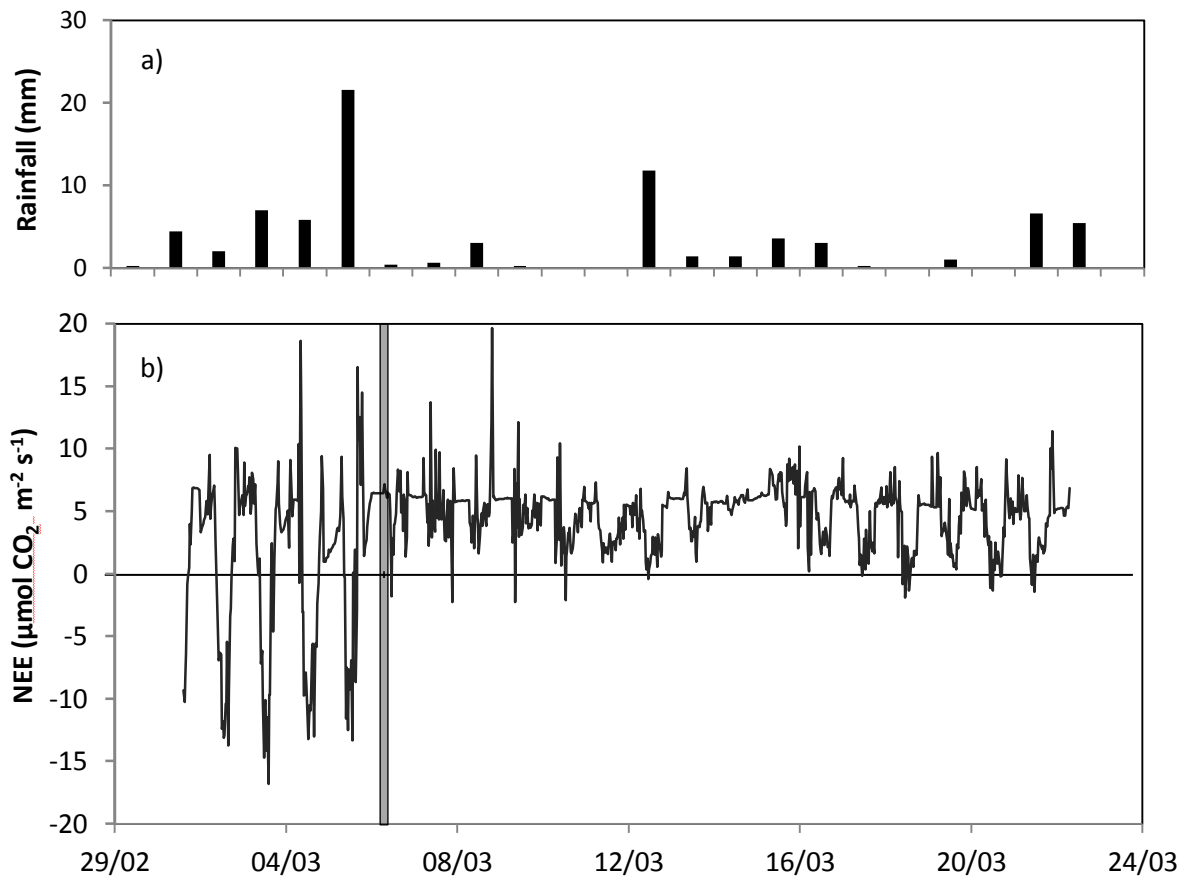


70 Figure 3

71

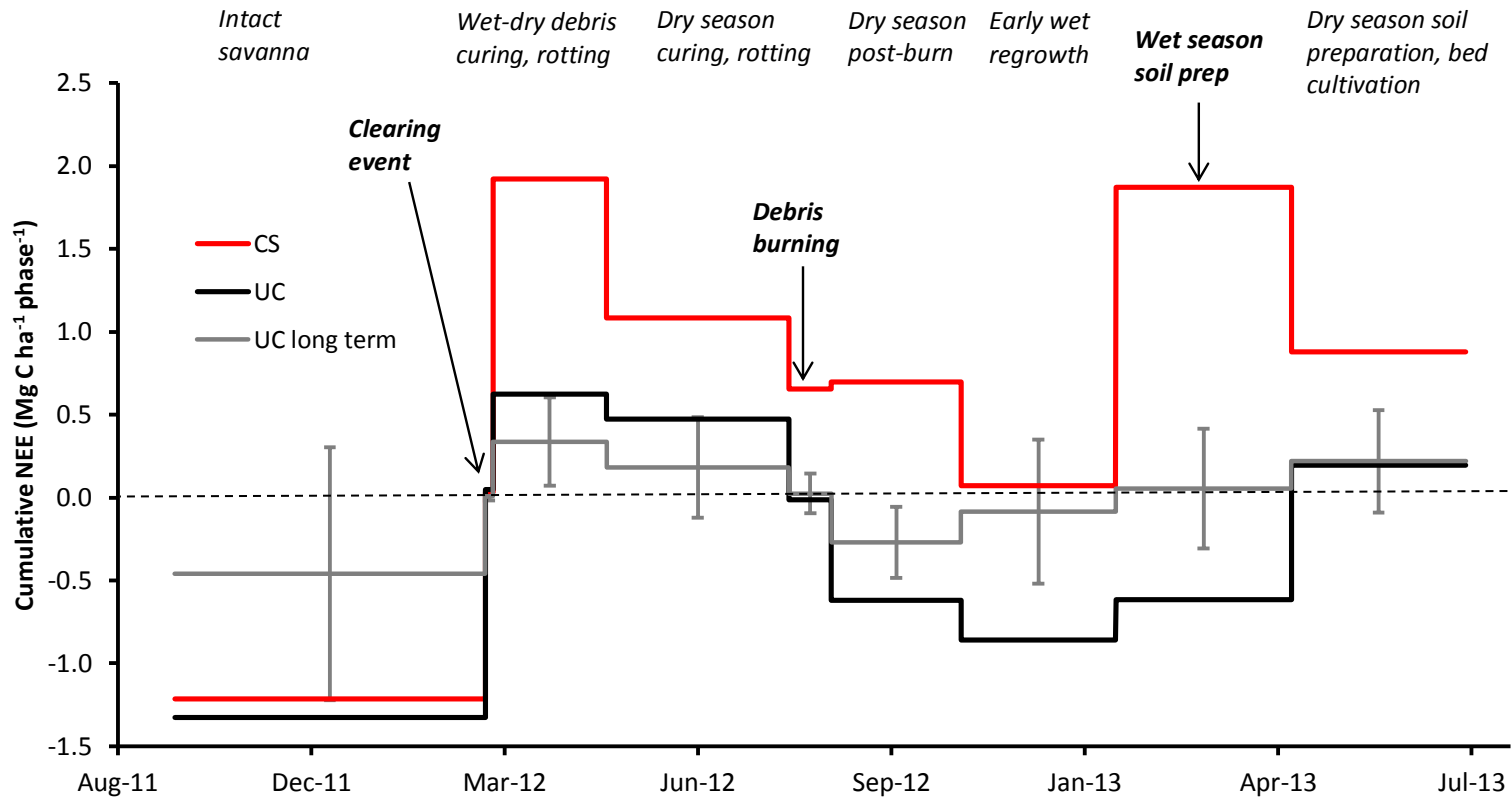
72

73





75 Figure 4



76

77

78 Plate 1  
79



80  
81  
82  
83

